

# 000 PARALLEL MULTIMODAL LARGE DIFFUSION LAN- 001 GUAGE MODELS FOR THINKING-AWARE EDITING AND 002 GENERATION 003

004 **Anonymous authors**  
005  
006

007 Paper under double-blind review  
008  
009

## 010 ABSTRACT 011

012 While thinking-aware generation aims to improve performance on complex tasks,  
013 we identify a critical failure mode where existing sequential, autoregressive ap-  
014 proaches can paradoxically degrade performance due to error propagation. To sys-  
015 tematically analyze this issue, we propose ParaBench, a new benchmark designed  
016 to evaluate both text and image output modalities. Our analysis using ParaBench  
017 reveals that this performance degradation is strongly correlated with poor align-  
018 ment between the generated reasoning and the final image. To resolve this, we  
019 propose a parallel multimodal diffusion framework that enables continuous, bidi-  
020 rectional interaction between text and images throughout the entire denoising tra-  
021 jectory. The model is trained with supervised finetuning and then further opti-  
022 mized by Parallel Reinforcement Learning (ParaRL), a novel strategy that applies  
023 semantic rewards along the trajectory to enforce cross-modal consistency. Experi-  
024 ments validate that our approach significantly improves cross-modal alignment  
025 and semantic consistency, achieving a 6.9% improvement in Output Alignment  
026 on ParaBench compared to the state-of-the-art model, Bagel, establishing a more  
027 robust paradigm for thinking-aware image synthesis.

## 028 1 INTRODUCTION 029

030 Recent advances in multimodal generative models have achieved remarkable progress in instruction-  
031 based image generation and editing (Esser et al., 2024a; Labs, 2024; Wei et al., 2024; Liu et al.,  
032 2025b). Given diverse textual prompts, these models can produce visually coherent and semantically  
033 aligned results across a wide range of tasks. However, these models often struggle with **complex**  
034 **instructions that require reasoning over world knowledge**, frequently leading to incorrect editing  
035 and generation (Wu et al., 2025c; Niu et al., 2025; Zhao et al., 2025). To mitigate this gap, recent  
036 studies have introduced intermediate reasoning steps before visual generation (Fang et al., 2025;  
037 Jiang et al., 2025a; Deng et al., 2025a). In these approaches, textual reasoning is first performed  
038 to guide subsequent image synthesis and editing. Such explicit reasoning has proven effective in  
039 improving the quality and consistency of image editing and generation (Deng et al., 2025a).  
040

041 Despite the general effectiveness of incorporating a reasoning process prior to image synthesis, we  
042 observe a counterintuitive and critical phenomenon. On certain benchmarks (Wu et al., 2025c),  
043 the inclusion of reasoning can in fact **reduce the semantic fidelity of the generated images** (Figure  
044 1(c)). This raises a crucial question: *What underlies this performance degradation?*

045 To investigate this, we introduce *ParaBench*, our new benchmark designed to evaluate the output  
046 alignment between a model’s generated reasoning and its final image. Using ParaBench to eval-  
047 uate the state-of-the-art model Bagel (Deng et al., 2025a), we find a strong correlation: performance  
048 degradation occurs precisely in categories where output alignment is weakest (Figure 1(d)). We  
049 attribute this to the compounding errors inherent in sequential autoregressive models, where am-  
050 biguous or incomplete reasoning provides unreliable guidance for the subsequent image generation,  
051 ultimately degrading the final output.

052 Thus, while pre-reasoning can in principle enhance multimodal generation, its reliance on an autore-  
053 gressive pipeline makes the process vulnerable to error accumulation and semantic drift. Recently,  
054 another line of work has explored discrete diffusion models for text or image generation (Nie et al.,

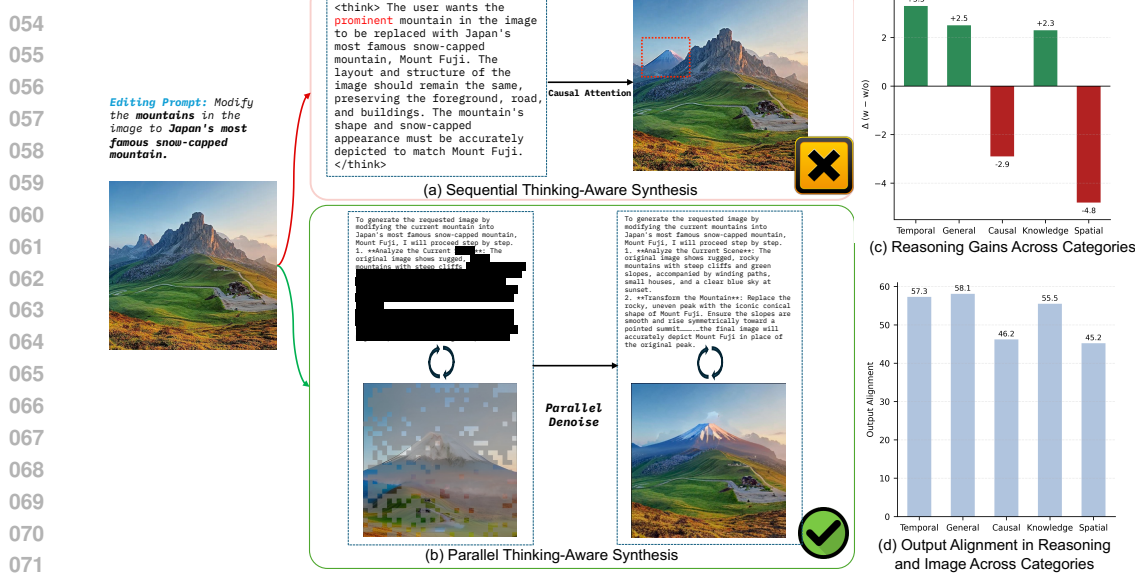


Figure 1: Sequential vs. parallel thinking-aware image editing and analysis. (a) Sequential generation (Bagel, GPT4o) may suffer from vague or incorrect reasoning. (b) Parallel generation aligns text and image at each denoising step, reducing hallucination and errors. (c) Quantitative comparison shows reasoning can degrade performance in certain categories. (d) Poorer categories also exhibit weaker reasoning—image alignment, highlighting the need for stronger cross-modal alignment.

2025; Yang et al., 2025a; Ye et al., 2025a), which remove the token-by-token constraint of autoregression and instead employ confidence-based sampling to achieve greater global consistency.

Inspired by these advances, we ask: **What if multimodal models could generate text and images in parallel?** Such a paradigm directly addresses the limitations of AR reasoning: text and images can attend to each other at every denoising step, avoiding the propagation of hallucinations and vague priors while grounding textual descriptions in visual evidence.

Building on this insight, we propose a purely diffusion-based framework for *parallel text–image generation*, where cross-modal interaction is maintained throughout the trajectory to ensure robust and semantically faithful multimodal editing and generation. (Figure 1) We begin by performing supervised fine-tuning of MMAoDA (Yang et al., 2025a) on our collected thinking-aware image synthesis data. This parallel version, MMAoDA-Parallel, demonstrates higher output consistency compared to sequential baselines. Importantly, such consistency is observed not only in the final outputs but also **throughout the generation trajectory**. Building on this foundation, we further introduce *Parallel Reinforcement Learning(ParaRL)*, which optimizes alignment along the denoising trajectory. Instead of focusing solely on the final outcome, ParaRL incorporates stepwise semantic supervision to refine alignment at the trajectory level.

Extensive quantitative and qualitative results validate the effectiveness of MMAoDA-Parallel for thinking-aware image editing and generation, and further highlight the additional gains achieved through ParaRL. On our ParaBench, MMAoDA-Parallel achieves 6.9% improvement over Bagel, and comparable image-only synthesis performance. Our contributions can be summarized as follows:

1. **In-depth Benchmarking and Analysis of Thinking-aware Image Synthesis.** We propose ParaBench, which systematically evaluates thinking-aware image generation and editing, focusing on text and image quality and their alignment.
2. **Parallel Multimodal Diffusion Framework.** We propose a purely discrete diffusion-based approach for parallel thinking-aware image editing and generation, which enables bidirectional attention between modalities at every denoising step and effectively alleviates the error accumulation of autoregressive pipelines.
3. **Parallel Reinforcement Learning.** We introduce a parallel reinforcement learning strategy, *ParaRL*, which assigns semantic rewards along the denoising trajectory, further enhancing alignment between the output modalities and the overall performance.

108  
 109  
 110  
 111  
 112  
 113  
 114  
 115  
 116  
 117  
 118  
 119  
 120  
 121  
 122  
 123  
 124  
 125  
 126  
 127  
 128  
 129  
 130  
 131  
 132  
 133  
 134  
 135  
 136  
 137  
 138  
 139  
 140  
 141  
 142  
 143  
 144  
 145  
 146  
 147  
 148  
 149  
 150  
 151  
 152  
 153  
 154  
 155  
 156  
 157  
 158  
 159  
 160  
 161

4. **Extensive Evaluation and State-of-the-Art Alignment.** Our comprehensive experiments validate the framework, establishing state-of-the-art performance among open-source models with a 6.9% gain in Output Alignment over Bagel on our ParaBench benchmark, while maintaining comparable performance on single-modality metrics.

## 2 RELATED WORK

Recent progress in multimodal models for image understanding, generation, and editing has been rapid, yet most approaches remain constrained to single-modal generation conditioned on multiple modalities (Esser et al., 2024b; Wu et al., 2025a; Labs et al., 2025; Bai et al., 2025). To improve the accuracy and fidelity of multimodal generation, a growing line of work has explored introducing a textual *Chain-of-Thought* reasoning process before image generation or editing. We refer to this paradigm as **thinking-aware image generation and editing**. For instance, early efforts such as Chameleon (Team, 2024) and Mogao (Liao et al., 2025) investigated interleaved generation, enabling interleaving sequences of text and image tokens. Image-CoT (Guo et al., 2025b) and GoT (Fang et al., 2025) incorporated CoT reasoning prior to image synthesis, demonstrating that reasoning traces can enhance generation quality. Bagel (Deng et al., 2025a) further extended this idea by integrating chain-of-thought reasoning into both image generation and editing, enabling more flexible and semantically aligned outputs. Building on this direction, follow-up works such as OmniGen2 (Wu et al., 2025b) and IRG (Huang et al., 2025a) introduced reflective reasoning after image generation, using multi-turn textual feedback to iteratively refine visual outputs. Most existing methods, however, rely on a sequential autoregressive interleaved pipeline, which could limit direct cross-modal interaction and make the model prone to error accumulation from imperfect reasoning traces. Exploring a parallel generation framework that enables more interaction within output modalities is still lacking in this scenario. (More related work can be found in Appendix C).

## 3 METHOD

### 3.1 FINDINGS AND BENCHMARKING ON THINKING-AWARE SYNTHESIS

To investigate whether pre-generation reasoning genuinely enhances performance, we conduct a controlled study on image editing tasks, which provides a clearer instruction-grounded evaluation than naive synthesis. We sample inputs from established benchmarks (Wu et al., 2025c; Zhao et al., 2025) and generate paired outputs using Bagel (Deng et al., 2025a)—one of the few open-source unified models supporting thinking-aware generation—with and without thinking. We report the average editing evaluation metrics in Kris-Bench (Wu et al., 2025c) in Figure 1(c) and also Table 1.

**Findings.** While the reasoning step enhanced performance on most tasks, a notable countertrend emerged: performance declined in a significant subset of cases, about 23%, particularly in complex compositional edits. A closer analysis reveals that these failures often stemmed from low-quality or vague reasoning text, which misguides the image generation process. This exposes a critical gap in existing protocols: they evaluate the final image but ignore the quality of the intermediate reasoning—the other generated modality.

**Benchmarking mixed modalities.** This analysis reveals a fundamental limitation in current evaluation paradigms: existing benchmarks (Wu et al., 2025c; Zhao et al., 2025; Ghosh et al., 2023) only evaluate images, ignoring the quality of the reasoning itself and its consistency with the image. To address this gap, we introduce **ParaBench**, a new benchmark specifically designed for the comprehensive evaluation of thinking-aware image synthesis. ParaBench comprises 300 challenging prompts, split into 200 for editing and 100 for generation. The editing prompts are meticulously curated to test a wide spectrum of abilities, covering not only general operations (e.g., add, remove, replace) but also complex tasks requiring reasoning. The 100 generation prompts focus on open-ended creative synthesis of complex scenes. We evaluate models on ParaBench using an GPT-4.1 across six fine-grained aspects: for the textual output, we assess Text Quality and Text Alignment; for the visual output, we evaluate Image Quality, Image Alignment, and Image Consistency; and finally, the overall Output Alignment between them. More details are included in Appendix G.

To demonstrate ParaBench’s diagnostic capabilities, we apply it to a representative baseline, Bagel. While full quantitative results are presented in Sec A, Table 1 highlights a crucial finding by focusing

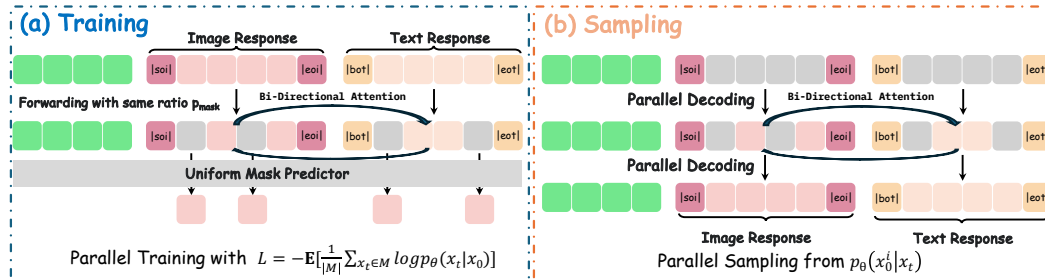
162 Table 1: Bagels’ performance comparison on ParaBench editing tasks with and without thinking.  
 163 We also report the reasoning quality (Text Qual.) and cross-modal alignment (Output Align.).

164 Editing Category	165 w/o Thinking	166 w/ Thinking	167 $\Delta$ (w/ - w/o)	168 Text Qual. $\uparrow$	169 Output Align. $\uparrow$
170 Temporal	171 72.3	172 75.6	173 +3.3	174 92.6	175 57.3
176 General	177 68.9	178 71.4	179 +2.5	180 86.2	181 58.1
182 Causal	183 70.1	184 67.2	185 -2.9	186 75.3	187 46.2
188 Knowledge	189 74.5	190 76.8	191 +2.3	192 87.8	193 55.5
195 Spatial	196 69.8	197 65.0	198 -4.8	199 73.2	200 45.2

201 on two key metrics: **Text Quality** and **Output Alignment**. The results reveal a clear correlation  
 202 between the quality of the reasoning step and the final performance. Notably, the categories that  
 203 exhibited performance degradation also suffered from significant drops in both reasoning quality  
 204 and reasoning-image synergy. This pattern strongly suggests that poor reasoning does not merely  
 205 fail to provide helpful guidance but actively misleads the generation process, validating the necessity  
 206 of explicitly improving the synergy between text and image generation.

207 **Motivations on parallel multimodal diffusion.** Our benchmarking results reveal a critical limitation  
 208 in current thinking-aware generation: the sequential generation paradigm, where reasoning  
 209 precedes image synthesis, creates a rigid dependency that can propagate errors and limit cross-modal  
 210 synergy. When reasoning quality degrades, it directly undermines the subsequent image generation,  
 211 as demonstrated by the correlated performance drops in spatial and temporal editing tasks. To ad-  
 212 dress this fundamental issue, we propose a parallel unified multimodal diffusion framework that  
 213 enables simultaneous generation of both reasoning text and images, fostering genuine multimodal  
 214 collaboration while eliminating the error propagation inherent in sequential approaches.

### 215 3.2 BASIC ALGORITHM AND ARCHITECTURE



216 Figure 2: Parallel Generation Architecture: During (a) training, image and text responses are masked  
 217 and predicted in parallel with a uniform mask predictor, optimized by the masked token likelihood  
 218 objective. During (b) sampling, the model performs parallel decoding to generate both image and  
 219 text responses jointly, enabling efficient multimodal response generation.

220 Discrete diffusion models have demonstrated strong performance for both image and text genera-  
 221 tion (Bai et al., 2024; Nie et al., 2025; Zhu et al., 2025). Building on the unified discrete-diffusion  
 222 view, MMaDA (Yang et al., 2025a) proved that a single diffusion framework can jointly model  
 223 multiple modalities, yet its decoding remained *sequential* across modalities. To overcome this lim-  
 224 itation, we propose a *parallel* multimodal diffusion framework that: (i) represents all modalities as  
 225 discrete tokens, (ii) arranges them in an interleaved sequence with bidirectional attention, and (iii)  
 226 employs a single mask predictor shared across modalities, enabling synchronous denoising for both  
 227 text and images. An overview of this framework is shown in Figure 2.

228 **Interleaved discrete sequence layout.** Following the MMaDA framework (Yang et al., 2025a),  
 229 we process both text and images within a unified discrete token space. Specifically, we tokenize  
 230 text using the LLaDA tokenizer (Nie et al., 2025) and encode images into a grid of discrete visual  
 231 tokens using a pretrained MAGVIT-v2 (Yu et al., 2023) quantizer. These tokenized modalities are  
 232 then serialized into a single interleaved sequence, using explicit sentinels and task tags to enable full  
 233 bidirectional cross-modal attention:

234 Input : <|task|><|soi|>[img]<|eof|><|bos|>[text]<|eos|>  
 235 Output: <|soi|>[output img]<|eof|><|bos|>[output text]<|eos|>

216 During training, we concatenate the input and output templates into one sequence so that the model  
 217 can attend from outputs to inputs within a single context. The task token  $<|\text{task}|>$  is instantiated  
 218 differently depending on the scenario, with  $<|\text{thinkgen}|>$  used for thinking-aware generation  
 219 and  $<|\text{thinkedit}|>$  used for thinking-aware editing. This single-sequence design eliminates the  
 220 ordering asymmetry and exposure bias introduced by autoregressive cross-modal pipelines.  
 221

222 **Training objective.** Let  $x_0 \in \{1, \dots, V\}^L$  denote the concatenated training sequence (input part  
 223 followed by output part), where  $L$  is the total number of tokens in the sequence. We keep the input  
 224 part static and apply noise only to the output part. At a sampled timestep  $t \in \{1, \dots, T\}$ , for each  
 225 token in the *output* part we replace it with `[MASK]` with probability  $\beta_t$  and keep it unchanged with  
 226 probability  $1 - \beta_t$ ; tokens in the *input* part are left unchanged:  
 227

$$x_t^{(i)} = \begin{cases} x_0^{(i)} & \text{if } i \text{ in input,} \\ x_0^{(i)} \text{ with prob. } (1 - \beta_t), \text{ [MASK] with prob. } \beta_t & \text{if } i \text{ in output.} \end{cases} \quad (1)$$

228 Equivalently, for positions in the output, the absorbing-state marginal after  $t$  steps is  $q(x_t \mid x_0) =$   
 229  $\alpha_t x_0 + (1 - \alpha_t) \mathbf{m}$  where  $\alpha_t = \prod_{k=1}^t (1 - \beta_k)$ , and  $\mathbf{m}$  is the one-hot distribution of `[MASK]`.  
 230

232 The parallel diffusion model  $p_\theta(\cdot \mid x_t)$  is formulated as a unified masked-token predictor over  
 233 the joint vocabulary of text and image tokens. Let  $i \in 1, \dots, L$  denote token positions in the  
 234 concatenated input–output sequence. Since only the output segment is noised during diffusion, the  
 235 model predicts ground-truth tokens  $x_0$  at the currently masked positions within this segment. To  
 236 better balance the training dynamics across modalities, we make the timestep-dependent loss weight  
 237 modality-specific: tokens in the *output image* segment and the *output text* segment are assigned  
 238 separate weights,  $w_{\text{img}}(t)$  and  $w_{\text{text}}(t)$ . For compactness, we write the objective using a unified  
 239 token-aware weight function  $w(t, i)$ . We optimize a timestep-reweighted cross-entropy:  
 240

$$\mathcal{L}_{\text{parallel}}(\theta) = -\mathbb{E}_{t, x_0, x_t} \left[ \sum_{i=1}^L w(t, i) \mathbf{1}[x_t^{(i)} = \text{[MASK]}] \log p_\theta(x_0^{(i)} \mid x_t) \right], \quad (2)$$

242 where  $\mathbf{1}[\cdot]$  is the indicator function and  
 243

$$w(t, i) = \begin{cases} w_{\text{img}}(t), & \text{if } i \text{ lies in the } \textit{output image} \text{ segment,} \\ w_{\text{text}}(t), & \text{if } i \text{ lies in the } \textit{output text} \text{ segment.} \end{cases}$$

244 We empirically find that applying a timestep-dependent weighting  $w_{\text{text}}(t) = 1/t$  for text tokens  
 245 and a constant weighting  $w_{\text{img}}(t) = 1$  for image tokens substantially stabilizes the training of image  
 246 quality and output alignment. Additional preliminaries and ablations are detailed in Appendix D.  
 247

248 **Parallel denoising with dual schedulers.** Decoding proceeds along a shared diffusion time axis  
 249  $t_T \rightarrow \dots \rightarrow t_0$ . We define two modality-specific schedulers,  $u_{\text{img}}(t), u_{\text{text}}(t) \in [0, 1]$ , which specify  
 250 the target proportion of unmasked tokens at step  $t$ . At each reverse step: (i) the model jointly predicts  
 251 distributions for all currently masked positions; (ii) for each modality, a fraction of tokens is sam-  
 252 pled (e.g., via confidence-based sampling), while the remaining positions are retained as `[MASK]`.  
 253 Because attention is bidirectional across the *entire* sequence, text and image can inform each other  
 254 at every step of decoding. In our experiments, the text schedule is implemented as a fully linear  
 255 reveal schedule combined with semi-autoregressive confidence-based decoding Nie et al. (2025),  
 256 while the image schedule follows a cosine reveal schedule with global confidence-based decoding.  
 257 More details can be found in Appendix E.  
 258

### 259 3.3 POST TRAINING WITH PARALLEL REINFORCEMENT LEARNING

260 **Supervised Finetuning for Parallel Synthesis** A key challenge in our approach is that existing gen-  
 261 eration and editing datasets lack the reasoning traces required for our parallel synthesis framework.  
 262 To address this, we construct a suitable training dataset by first aggregating samples from various  
 263 sources. For each sample comprising an input image (for editing tasks), an instruction, and the final  
 264 output image, we employ a multimodal LLM (Qwen-2.5-VL in our implementation) to generate a  
 265 corresponding reasoning trace. Further details on the dataset construction process, including the  
 266 sources and categories, are provided in Appendix F. We then use this dataset to perform supervised  
 267 fine-tuning on MMA (Yang et al., 2025a). This process adapts it into a parallel variant capable of  
 268 performing thinking-aware synthesis, where reasoning and generation occur concurrently.  
 269

270  
271  
272  
273  
274  
275  
276  
277  
278  
279

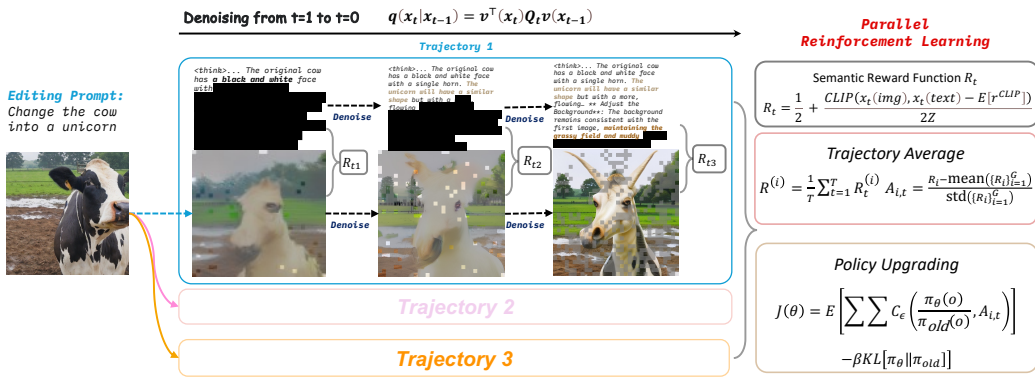


Figure 3: Overview of our proposed Parallel Reinforcement Learning (ParaRL). Rather than optimization only to the final denoised outputs, ParaRL introduces reward signals along the entire denoising trajectory, reinforcing semantic alignment consistently throughout the generation process.

**Synergy along the denoising trajectory.** While analyzing generations from the finetuned model, we observe that certain semantic concepts emerge *syn-chronously* in text and image at intermediate denoising steps. As illustrated in Figure 4, when tasked to change a shirt to a “vibrant rainbow color,” the specific color words and their corresponding visual features appear at the same timestep. This observation leads to a key insight: cross-modal alignment is not an endpoint phenomenon but is progressively established **throughout the generation trajectory**. This implies that supervision applied to these intermediate steps, not just the final output, can further improve this alignment.

**Parallel reinforcement learning with trajectory optimization.** Building on this insight, we introduce Parallel Reinforcement Learning (ParaRL), a novel training paradigm that directly leverages this intermediate cross-modal synergy. Instead of rewarding only the final output, ParaRL uses the alignment between text and image tokens at each denoising step as a dense reward signal.

Specifically, for a given query  $Q$ , the generated response is a full trajectory  $\tau_i \triangleq (\tau_i(1), \dots, \tau_i(|\tau_i|))$ , where  $|\tau_i|$  is the total number of denoising steps and  $\tau_i(t)$  is the set of tokens decoded at step  $t$ . While this formulation provides a step-wise reward  $r_{i,t}$  for each intermediate response  $\tau_i(t)$ , optimizing over the entire dense trajectory is computationally prohibitive. To make training feasible, we adopt a sparse optimization strategy. During each online rollout, we pre-select sampling steps  $s$  and fix subset of step indices  $S \subset \{1, \dots, |\tau_i|\}$ ,  $|S| = s$  and only compute rewards  $r_{i,t}$  and their corresponding standardized advantages  $A_{i,t}$  for timesteps  $t \in S$ . We adopt a diffusion GRPO objective (Gong et al., 2025) that accommodates token-level likelihood ratios with advantages calculated at these sampled steps:

$$\mathcal{J}_{\text{policy}}(\theta) = \mathbb{E}_{\substack{Q \sim D_{\text{task}} \\ \{\tau_i\}_{i=1}^G \sim \pi_{\text{old}}(\cdot | Q)}} \left[ \sum_{i=1}^G \sum_{t \in S} \frac{1}{|\tau_i(t)|} \sum_{o \in \tau_i(t)} C_\epsilon \left( \frac{\pi_\theta(o | Q, \tau_i(1:t-1))}{\pi_{\text{old}}(o | Q, \tau_i(1:t-1))}, A_{i,t} \right) \right] - \beta \text{KL}[\pi_\theta \| \pi_{\text{old}}], \quad (3)$$

where  $C_\epsilon(r, A) \triangleq \min(rA, \text{clip}(r, 1 - \epsilon, 1 + \epsilon)A)$ . In this objective, the summation is performed over the sparsely sampled steps  $t \in S$ . The term  $o$  ranges over all tokens within the state  $\tau_i(t)$  at a sampled step  $t$ , and  $\tau_i(1:t-1)$  denotes the full history of tokens generated prior to step  $t$ . Finally,  $\pi_{\text{old}}$  is the behavior policy for generating rollouts, and  $\beta$  controls the KL penalty strength.

**Trajectory reward design.** In typical trajectory-level optimization frameworks, a well-trained process reward model (PRM) (Li & Li, 2024) or value function Wang et al. (2025) is often required, since intermediate partial outputs usually lack sufficient semantic information for reliable evaluation. Surprisingly, in our parallel text–image generation setting, we find that intermediate fragments

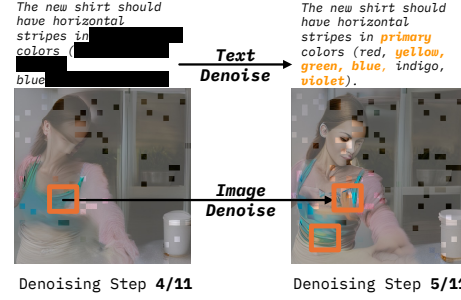


Figure 4: Synergy of sampling. Given the prompt: “change the blue shirt to a vibrant rainbow color,” the specific color decoding in text and image emerges at the same step.

324 are already semantically meaningful. For instance, even partially decoded text tokens often reveal  
 325 enough semantic cues to compute alignment with the simultaneously generated image content, as  
 326 illustrated in Fig. 3. This observation allows us to bypass the need for a dedicated PRM: we directly  
 327 employ *semantic alignment* between text and image as the reward signal.

328 Unlike tasks with binary rewards (e.g., mathematical reasoning), our cross-modal alignment ob-  
 329 jective provides a continuous reward signal. However, the raw CLIP score, which serves as our  
 330 reward source, can exhibit high variance and an arbitrary scale, making it unstable for direct use  
 331 in reinforcement learning. To ensure training stability, we therefore apply a normalization scheme  
 332 inspired by prior work in RL with continuous rewards (Liu et al., 2025a). We begin by estimating  
 333 the mean  $\mu_{\text{CLIP}}$  and standard deviation  $\sigma_{\text{CLIP}}$  of CLIP scores across the training distribution, which  
 334 we compute on a random 1% subset of the data. Let  $c_{i,t} = R^{\text{CLIP}}(\text{text}(\tau_i(t)), \text{image}(\tau_i(t)))$  be the  
 335 raw CLIP score for the content generated at step  $t$ . We first standardize this score to obtain  $\hat{c}_{i,t}$  using  
 336  $\hat{c}_{i,t} = \frac{c_{i,t} - \mu_{\text{CLIP}}}{\sigma_{\text{CLIP}}}$ . This standardized score is then clipped to the range  $[-1, 1]$  and linearly rescaled to  
 337 yield the final reward  $R_{i,t}$ , which is bounded within  $[0, 1]$ :

$$R_{i,t} = \frac{1}{2} (1 + \text{clip}(\hat{c}_{i,t}, -1, 1)) \quad (4)$$

341 The corresponding advantages  $A_{i,k}$  used in Eq. 3 are then obtained by standardization over the  
 342 rollouts:  $A_{i,t} = \frac{R_{i,t} - \text{mean}(\{R_{j,t}\}_{j=1}^G)}{\text{std}(\{R_{j,t}\}_{j=1}^G)}$

## 344 4 EXPERIMENTS

### 345 4.1 IMPLEMENTATION DETAILS

348 **Training and datasets.** Our final model, MMaDA-Parallel, is trained in a two-stage process. We  
 349 begin with supervised finetuning (SFT) on the MMaDA-MixCoT model, which integrates a LLaDA-  
 350 8B text backbone with a MagVIT-v2 image tokenizer. For this stage, we construct a new dataset of  
 351 150K thinking-aware image editing and generation pairs, meticulously sourced and filtered from  
 352 multiple existing benchmarks. In the second stage, we apply reinforcement learning with a GRPO-  
 353 based objective. To enhance training efficiency, this RL stage focuses on the most challenging 10%  
 354 of the SFT examples, optimizing the policy online to improve cross-modal semantic alignment.  
 355 More details of the dataset and training details can be found in Appendix F and H.

356 **Evaluation setup.** We conduct our primary evaluation on the ParaBench benchmark, which was  
 357 introduced in the Method section. We employ an LLM-as-a-judge framework (GPT-4.1) to assess  
 358 performance across the six fine-grained metrics previously described, covering text quality, image  
 359 fidelity, and cross-modal alignment. The prompts used for the LLM judge are detailed in the Ap-  
 360 pendix G. Our MMaDA-Parallel is compared against state-of-the-art thinking-aware models, includ-  
 361 ing Bagel (Deng et al., 2025a), GPT-4o, and Gemini-2.5, as well as leading image-only generators  
 362 like Qwen-Image (Wu et al., 2025a), Qwen-Image-Edit (Wu et al., 2025a), Flux.1-dev (Labs, 2024)  
 363 and Flux.1-Kontext (Labs et al., 2025).

### 365 4.2 MAIN RESULTS

367 Table 2 reports the overall performance on our ParaBench benchmark. Our proposed method,  
 368 MMaDA-Parallel, achieves the highest *Output Alignment* among all open-source models, confirm-  
 369 ing the effectiveness of its parallel multimodal decoding and trajectory-level optimization. In terms  
 370 of general text and image quality, MMaDA-Parallel performs on par with Bagel, despite Bagel be-  
 371 ing trained on a dataset nearly three orders of magnitude larger. Compared to leading closed-source  
 372 models like GPT-4o and Gemini-2.5, MMaDA-Parallel substantially narrows the gap in alignment  
 373 metrics while maintaining competitive text and image quality, demonstrating remarkable data effi-  
 374 ciency. Furthermore, the results indicate that our ParaRL stage consistently improves output text-  
 375 image consistency, suggesting that trajectory-level optimization effectively strengthens cross-modal  
 376 grounding throughout the generation process.

377 In addition, we provide a qualitative comparison with open-source models in Figure 5, showcasing  
 examples of both editing and generation. A key observation is that MMaDA-Parallel produces more

378 **Table 2: Main results on *ParaBench*.** Evaluation across all editing and generation tasks. For  
 379 non-thinking image editing or generation models, text evaluation and output alignment cannot be  
 380 computed.

381 Model	382 Text Qual.	383 Text Align.	384 Image Cons.	385 Image Align.	386 Image Qual.	387 Output Align.	388 Overall
<b>Open-source models (Non-thinking)</b>							
383 Flux-1-Dev	-	-	-	65.2	77.5	-	-
384 Qwen-Image	-	-	-	67.2	<b>84.2</b>	-	-
385 Flux-1-Kontext	-	-	77.9	65	84	-	-
386 Qwen-Image-Edit	-	-	78.2	73.5	84.1	-	-
387 Bagel (w/o think)	-	-	72.2	50.3	80.1	-	-
<b>Closed-source models</b>							
388 GPT-4o	92.5	93.4	86.2	<b>85.7</b>	88.1	<b>69.5</b>	<b>85.9</b>
389 Gemini-2.5	<b>94.1</b>	<b>95.2</b>	<b>88.5</b>	76.2	<b>90.2</b>	63.4	84.6
<b>Open-source models (Thinking-aware)</b>							
390 Bagel (w/ think)	<b>82</b>	70.5	<b>76.7</b>	<b>63.4</b>	<b>81.5</b>	<b>52.9</b>	71.2
391 Show-o* (tuned)	75.2	<u>70.7</u>	69.1	57.5	78.5	48.9	66.6
392 MMA-Parallel w/o ParaRL	76.5	70.4	70.5	58.2	80.5	51.5	67.9
393 MMA-Parallel w/ ParaRL	<u>80.4</u>	<b>71</b>	<u>73.4</u>	<u>63.2</u>	<u>81.2</u>	<b>59.8</b>	<b>71.5</b>

393 precise and descriptive reasoning traces. This enhanced reasoning leads to superior visual fidelity  
 394 in the final image. For instance, our model accurately renders complex instructions like a "melting  
 395 cake" and correctly applies causal reasoning to depict "withered grass." Moreover, MMA-Parallel  
 396 demonstrates stronger compositional abilities, particularly in counting, correctly generating "three  
 397 people" or "two faces of a clock" where Bagel often fails. In contrast, Bagel's reasoning in these  
 398 challenging cases tends to be vague or omits crucial details, leading to inaccurate image synthesis.  
 399 These results further underscore MMA-Parallel's capability for advanced thinking-aware editing  
 400 and generation, driven by better-aligned semantic information.

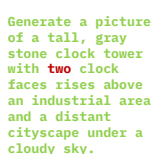
401 <b>Input</b>	402 <b>Bagel (w/ think)</b>	403 <b>MMA-Parallel</b>
404 	405 The question image shows a chocolate cake placed outdoors under sunlight, with a natural and serene background. The question text asks to display the cake melting in hot sunlight. The model should analyze the scene and determine the cake appears to be melting due to the heat. To achieve the requested display of the cake melting in hot sunlight, I'll start by analyzing the current state of the cake in the question image. The cake appears intact with a smooth surface and a dark chocolate glaze. The lighting is bright, suggesting a sunny day. The goal is to simulate the melting effect as described in the question. Firstly, I need to transform the cake, appearing as a solid chocolate cake, into a liquid state with a smooth, fluid surface. The top portion of the cake will lose its crisp edges and become soft and malleable. The lighting should show signs of the cake's weight, with a of the cake sliding off the plate. To enhance the melting effect, I'll consider the lighting conditions. The bright green grass and blue sky in the background will provide a strong contrast to the melting cake. The bright sunlight will be softened to simulate the intense sunlight hitting the cake, emphasizing the melting effect. The final image will show the cake melting in hot sunlight.	406 
407 	408 The question image shows a healthy, upright plant with vibrant green leaves under bright sunlight, indicating it is well-hydrated and thriving. The question text asks to show the plant wilting due to lack of water, which suggests the user wants a visual representation of the plant's condition when dehydrated. To create the answer image, I would imagine the plant drooping and losing its upright posture, with its curling or turning yellowish-brown, which are typical signs of dehydration. The lighting should remain consistent with the original image, maintaining the garden setting and bright sunlight to emphasize the contrast between the healthy and dehydrated plant. The answer text would describe the plant's dehydrated state, focusing on the drooping posture. The final image should clearly show the plant's transition from vitality to distress, aligning with the user's request.	409 
410 	411 The user wants the beer replaced with a smaller cup of coffee while keeping the laptop and its green keyboard. The image layout and other colors of the image should remain the same, with the cup of coffee placed in the same position as the beer. The keyboard color should be adjusted to gray to match the user's request.	412 
413 	414 The image should depict a sunny park scene where one person is actively throwing a frisbee, while the other two observe or prepare to catch it, showcasing a casual and playful atmosphere. Here's the finished detailed prompt: A vibrant, sunny park scene with a grassy field and playful atmosphere, with one person actively throwing a frisbee, while the other two observe or prepare to catch it. The park is lush with green grass, scattered trees, and a clear blue sky overhead. The individuals are dressed in casual athletic attire, such as shorts and t-shirts, and their expressions convey enjoyment and engagement. The image should emphasize the texture of the grass, the frisbee's motion blur, and the interplay of light and shadow, creating a vivid and immersive scene.	415 
416 	417 The model should generate an image featuring the Big Ben clock tower in London, showing its height, stone structure, and the surrounding urban environment. The expanded prompt follows: A majestic, tall, gray stone clock tower, Big Ben in London, standing prominently above an industrial area with modern skyscrapers in the background. The scene is set against a distant cityscape with an overcast sky, creating a dramatic, atmospheric scene. The image should be ultra-realistic, with intricate details of the tower's stone texture, the clock faces, and the surrounding urban environment, capturing the grandeur and historical significance of the landmark.	418 

Figure 5: Qualitative results in comparison with Bagel.

432 

### 4.3 ANALYSIS OF KEY CONTRIBUTIONS

433 Table 3: Parallel vs sequential decoding.

Denoising	Text Align.	Image Align.	Output Align.
Sequential	70.6	56.1	48.9
Parallel	<b>70.4</b>	<b>58.2</b>	<b>51.5</b>

437 Table 4: Output vs trajectory-level RL.

Model	Text Align.	Image Align.	Output Align.
before RL	70.4	58.2	51.5
w/ Output-level RL	70.7	62.3	53.6
w/ ParaRL (Ours)	<b>71</b>	<b>63.2</b>	<b>59.8</b>

438 Table 5: Ablation on sampling steps  $s$  in ParaRL.

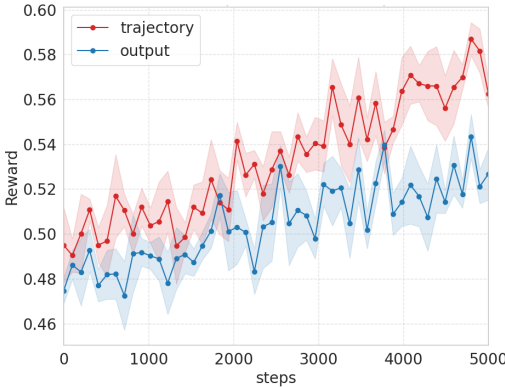
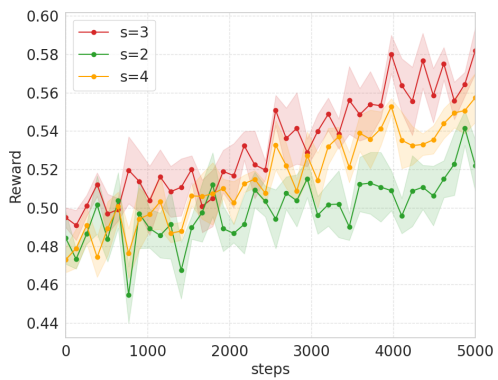
ParaRL $s$	Text Qual.	Text Align.	Image Cons.	Image Align.	Image Qual.	Output Align.	Overall
Before RL	76.5	70.4	70.5	58.2	80.5	51.5	67.9
ParaRL $s=2$	77.9	70.3	71.5	62.8	80.7	53.6	68.6
ParaRL ( $s=3$ ) (default)	<b>80.4</b>	<b>71.0</b>	<b>73.4</b>	<b>63.2</b>	<b>81.2</b>	<b>59.8</b>	<b>71.5</b>
ParaRL ( $s=4$ )	<b>80.5</b>	70.8	<u>73.2</u>	<b>63.5</b>	<u>80.8</u>	<u>58.7</u>	<u>71.3</u>

439 After presenting the overall results, we now return to the two central research questions that motivated our work: **RQ1**: Does parallel denoising improve generation quality compared with sequential denoising? **RQ2**: Does trajectory-level finetuning improve over output-level finetuning?

440 **The Benefit of Parallel Decoding (RQ1).** We compare our model against a sequential baseline (*MMA-Sequential*) that generates text before images. During training, noise was applied to only one modality at a time to align with this sequential inference process. Table 3 shows our parallel framework substantially outperforms this baseline on key alignment metrics, with comparable text and image quality. This result validates our core hypothesis: simultaneous, interactive decoding is crucial for reducing error propagation and producing coherent multimodal outputs.

441 **The Benefit of Trajectory-Level Optimization (RQ2).** We compare two reinforcement learning strategies: (i) *output-level RL*, where rewards are computed on the final generated sample, and (ii) our proposed *ParaRL* with trajectory-level finetuning, where rewards are aggregated across denoising steps. As shown in Table 4, trajectory-level optimization yields gains in text–image consistency and output alignment, and Figure 6 further shows that it enables more stable training dynamics.

442 Another key hyperparameter in this strategy is the number of sampled steps,  $s$ . We analyze its impact in Table 5 and report the training curve in Figure 7. We find that using  $s = 3$  or  $s = 4$  yields substantial improvements over  $s = 2$ , as a denser reward signal provides more stable guidance. We adopt  $s = 3$  in the final configuration for the best balance between performance and efficiency.

443 Figure 6: ParaRL reward training curve between  
444 trajectory and output level optimization.445 Figure 7: ParaRL reward training curve across  
446 different sampling steps of the trajectory.447 

## 5 CONCLUSION

448 In this work, we investigated a critical phenomenon where sequential thinking-aware models can 449 paradoxically suffer from performance degradation on complex tasks. We conducted an in-depth 450 analysis using our proposed ParaBench benchmark, which uniquely evaluates both output modalities, 451 and found a strong correlation between this degradation and poor alignment between the generated 452 modalities. To resolve this, we propose a parallel multimodal diffusion framework trained with 453 supervised finetuning and further optimized by Parallel Reinforcement Learning (ParaRL)—our 454 novel method of applying rewards along the entire denoising trajectory. Experiments validate that 455 our approach significantly improves cross-modal alignment and semantic consistency, establishing 456 a more robust paradigm for thinking-aware image synthesis.

486 

## 6 ETHICS STATEMENT

487  
488 This work advances research in text and image generation. We acknowledge that such models may  
489 be misused to create deceptive or harmful content, such as falsified images or misleading infor-  
490 mation. Our study is conducted for scientific purposes, and we encourage responsible use with  
491 appropriate safeguards to mitigate potential misuse.492  
493 

## 7 REPRODUCIBILITY STATEMENT

494  
495 We provide detailed training implementation details in Appendix H and our main training code in  
496 the supplementary. All code and data will be made public upon acceptance.497  
498 

## REFERENCES

500 Jacob Austin, Daniel D Johnson, Jonathan Ho, Daniel Tarlow, and Rianne Van Den Berg. Structured  
501 denoising diffusion models in discrete state-spaces. *Advances in neural information processing*  
502 *systems*, 34:17981–17993, 2021.503  
504 Jinbin Bai, Tian Ye, Wei Chow, Enxin Song, Xiangtai Li, Zhen Dong, Lei Zhu, and Shuicheng  
505 Yan. Meissonic: Revitalizing masked generative transformers for efficient high-resolution text-  
506 to-image synthesis. *arXiv preprint arXiv:2410.08261*, 2024.507 Shuai Bai, Keqin Chen, Xuejing Liu, Jialin Wang, Wenbin Ge, Sibo Song, Kai Dang, Peng Wang,  
508 Shijie Wang, Jun Tang, et al. Qwen2. 5-vl technical report. *arXiv preprint arXiv:2502.13923*,  
509 2025.510 Tim Brooks, Aleksander Holynski, and Alexei A Efros. Instructpix2pix: Learning to follow image  
511 editing instructions. In *Proceedings of the IEEE/CVF conference on computer vision and pattern*  
512 *recognition*, pp. 18392–18402, 2023.513  
514 Huiwen Chang, Han Zhang, Lu Jiang, Ce Liu, and William T Freeman. Maskgit: Masked generative  
515 image transformer. In *CVPR*, pp. 11315–11325, 2022.516  
517 Huiwen Chang, Han Zhang, Jarred Barber, AJ Maschinot, Jose Lezama, Lu Jiang, Ming-Hsuan  
518 Yang, Kevin Murphy, William T Freeman, Michael Rubinstein, et al. Muse: Text-to-image gen-  
519 eration via masked generative transformers. *arXiv preprint arXiv:2301.00704*, 2023.520 Junying Chen, Zhenyang Cai, Pengcheng Chen, Shunian Chen, Ke Ji, Xidong Wang, Yunjin Yang,  
521 and Benyou Wang. Sharegpt-4o-image: Aligning multimodal models with gpt-4o-level image  
522 generation. *arXiv preprint arXiv:2506.18095*, 2025a.523  
524 Liang Chen, Lei Li, Haozhe Zhao, Yifan Song, and Vinci. R1-v: Reinforcing super generalization  
525 ability in vision-language models with less than \$3. <https://github.com/Deep-Agent/R1-V>, 2025b. Accessed: 2025-02-02.526  
527 Ting Chen, Ruixiang Zhang, and Geoffrey Hinton. Analog bits: Generating discrete data using  
528 diffusion models with self-conditioning. *arXiv preprint arXiv:2208.04202*, 2022.529  
530 Chaorui Deng, Deyao Zhu, Kunchang Li, Chenhui Gou, Feng Li, Zeyu Wang, Shu Zhong, Weihao  
531 Yu, Xiaonan Nie, Ziang Song, et al. Emerging properties in unified multimodal pretraining. *arXiv*  
532 *preprint arXiv:2505.14683*, 2025a.533  
534 Yihe Deng, Hritik Bansal, Fan Yin, Nanyun Peng, Wei Wang, and Kai-Wei Chang. Openvlthinker:  
535 An early exploration to complex vision-language reasoning via iterative self-improvement, 2025b.  
536 URL <https://arxiv.org/abs/2503.17352>.537  
538 Patrick Esser, Sumith Kulal, Andreas Blattmann, Rahim Entezari, Jonas Müller, Harry Saini, Yam  
539 Levi, Dominik Lorenz, Axel Sauer, Frederic Boesel, et al. Scaling rectified flow transformers  
2024a. for high-resolution image synthesis. In *Forty-first international conference on machine learning*,

540 Patrick Esser, Sumith Kulal, Andreas Blattmann, Rahim Entezari, Jonas Müller, Harry Saini, Yam  
 541 Levi, Dominik Lorenz, Axel Sauer, Frederic Boesel, et al. Scaling rectified flow transformers  
 542 for high-resolution image synthesis. In *Forty-first international conference on machine learning*,  
 543 2024b.

544 Rongyao Fang, Chengqi Duan, Kun Wang, Linjiang Huang, Hao Li, Shilin Yan, Hao Tian, Xingyu  
 545 Zeng, Rui Zhao, Jifeng Dai, et al. Got: Unleashing reasoning capability of multimodal large  
 546 language model for visual generation and editing. *arXiv preprint arXiv:2503.10639*, 2025.

547 Dhruba Ghosh, Hannaneh Hajishirzi, and Ludwig Schmidt. Geneval: An object-focused framework  
 548 for evaluating text-to-image alignment. *Advances in Neural Information Processing Systems*, 36:  
 549 52132–52152, 2023.

550 Shansan Gong, Mukai Li, Jiangtao Feng, Zhiyong Wu, and LingPeng Kong. Diffuseq: Sequence to  
 551 sequence text generation with diffusion models. *arXiv preprint arXiv:2210.08933*, 2022.

552 Shansan Gong, Shivam Agarwal, Yizhe Zhang, Jiacheng Ye, Lin Zheng, Mukai Li, Chenxin An,  
 553 Peilin Zhao, Wei Bi, Jiawei Han, et al. Scaling diffusion language models via adaptation from  
 554 autoregressive models. *arXiv preprint arXiv:2410.17891*, 2024.

555 Shansan Gong, Ruixiang Zhang, Huangjie Zheng, Jiatao Gu, Navdeep Jaitly, Lingpeng Kong, and  
 556 Yizhe Zhang. Diffucoder: Understanding and improving masked diffusion models for code gen-  
 557 eration. *arXiv preprint arXiv:2506.20639*, 2025.

558 Shuyang Gu, Dong Chen, Jianmin Bao, Fang Wen, Bo Zhang, Dongdong Chen, Lu Yuan, and  
 559 Baining Guo. Vector quantized diffusion model for text-to-image synthesis. In *CVPR*, pp. 10696–  
 560 10706, 2022.

561 Daya Guo, Dejian Yang, Haowei Zhang, Junxiao Song, Ruoyu Zhang, Runxin Xu, Qihao Zhu,  
 562 Shirong Ma, Peiyi Wang, Xiao Bi, et al. Deepseek-r1: Incentivizing reasoning capability in llms  
 563 via reinforcement learning. *arXiv preprint arXiv:2501.12948*, 2025a.

564 Ziyu Guo, Renrui Zhang, Chengzhuo Tong, Zhizheng Zhao, Rui Huang, Haoquan Zhang, Manyuan  
 565 Zhang, Jiaming Liu, Shanghang Zhang, Peng Gao, et al. Can we generate images with cot? let's  
 566 verify and reinforce image generation step by step. *arXiv preprint arXiv:2501.13926*, 2025b.

567 Jonathan Ho, Ajay Jain, and Pieter Abbeel. Denoising diffusion probabilistic models. *Advances in  
 568 neural information processing systems*, 33:6840–6851, 2020.

569 Jixiang Hong, Yiran Zhang, Guanzhong Wang, Yi Liu, Ji-Rong Wen, and Rui Yan. Reinforcing mul-  
 570 timodal understanding and generation with dual self-rewards. *arXiv preprint arXiv:2506.07963*,  
 571 2025.

572 Wenzuan Huang, Shuang Chen, Zheyong Xie, Shaosheng Cao, Shixiang Tang, Yufan Shen, Qingyu  
 573 Yin, Wenbo Hu, Xiaoman Wang, Yuntian Tang, et al. Interleaving reasoning for better text-to-  
 574 image generation. *arXiv preprint arXiv:2509.06945*, 2025a.

575 Wenzuan Huang, Bohan Jia, Zijie Zhai, Shaosheng Cao, Zheyu Ye, Fei Zhao, Yao Hu, and Shaohui  
 576 Lin. Vision-r1: Incentivizing reasoning capability in multimodal large language models. *arXiv  
 577 preprint arXiv:2503.06749*, 2025b.

578 Mude Hui, Siwei Yang, Bingchen Zhao, Yichun Shi, Heng Wang, Peng Wang, Yuyin Zhou, and  
 579 Cihang Xie. Hq-edit: A high-quality dataset for instruction-based image editing. *arXiv preprint  
 580 arXiv:2404.09990*, 2024.

581 Dongzhi Jiang, Ziyu Guo, Renrui Zhang, Zhuofan Zong, Hao Li, Le Zhuo, Shilin Yan, Pheng-Ann  
 582 Heng, and Hongsheng Li. T2i-r1: Reinforcing image generation with collaborative semantic-level  
 583 and token-level cot. *arXiv preprint arXiv:2505.00703*, 2025a.

584 Jingjing Jiang, Chongjie Si, Jun Luo, Hanwang Zhang, and Chao Ma. Co-reinforcement learning  
 585 for unified multimodal understanding and generation. *arXiv preprint arXiv:2505.17534*, 2025b.

586

594 Black Forest Labs, Stephen Batifol, Andreas Blattmann, Frederic Boesel, Saksham Consul, Cyril  
 595 Diagne, Tim Dockhorn, Jack English, Zion English, Patrick Esser, Sumith Kulal, Kyle Lacey,  
 596 Yam Levi, Cheng Li, Dominik Lorenz, Jonas Müller, Dustin Podell, Robin Rombach, Harry Saini,  
 597 Axel Sauer, and Luke Smith. Flux.1 kontext: Flow matching for in-context image generation and  
 598 editing in latent space, 2025. URL <https://arxiv.org/abs/2506.15742>.

599 Shufan Li, Konstantinos Kallidromitis, Hritik Bansal, Akash Gokul, Yusuke Kato, Kazuki Kozuka,  
 600 Jason Kuen, Zhe Lin, Kai-Wei Chang, and Aditya Grover. Lavida: A large diffusion language  
 601 model for multimodal understanding. *arXiv preprint arXiv:2505.16839*, 2025.

602 Wendi Li and Yixuan Li. Process reward model with q-value rankings. *arXiv preprint  
 603 arXiv:2410.11287*, 2024.

604 Chao Liao, Liyang Liu, Xun Wang, Zhengxiong Luo, Xinyu Zhang, Wenliang Zhao, Jie Wu, Liang  
 605 Li, Zhi Tian, and Weilin Huang. Mogao: An omni foundation model for interleaved multi-modal  
 606 generation. *arXiv preprint arXiv:2505.05472*, 2025.

607 Jie Liu, Gongye Liu, Jiajun Liang, Yangguang Li, Jiaheng Liu, Xintao Wang, Pengfei Wan,  
 608 Di Zhang, and Wanli Ouyang. Flow-grpo: Training flow matching models via online rl. *arXiv  
 609 preprint arXiv:2505.05470*, 2025a.

610 Shiyu Liu, Yucheng Han, Peng Xing, Fukun Yin, Rui Wang, Wei Cheng, Jiaqi Liao, Yingming  
 611 Wang, Honghao Fu, Chunrui Han, Guopeng Li, Yuang Peng, Quan Sun, Jingwei Wu, Yan Cai,  
 612 Zheng Ge, Ranchen Ming, Lei Xia, Xianfang Zeng, Yibo Zhu, Binxing Jiao, Xiangyu Zhang,  
 613 Gang Yu, and Dixin Jiang. Step1x-edit: A practical framework for general image editing. *arXiv  
 614 preprint arXiv:2504.17761*, 2025b.

615 Shiyu Liu, Yucheng Han, Peng Xing, Fukun Yin, Rui Wang, Wei Cheng, Jiaqi Liao, Yingming  
 616 Wang, Honghao Fu, Chunrui Han, et al. Step1x-edit: A practical framework for general image  
 617 editing. *arXiv preprint arXiv:2504.17761*, 2025c.

618 Xiaoran Liu, Zhigeng Liu, Zengfeng Huang, Qipeng Guo, Ziwei He, and Xipeng Qiu. Longllada:  
 619 Unlocking long context capabilities in diffusion llms. *arXiv preprint arXiv:2506.14429*, 2025d.

620 Yuqi Liu, Bohao Peng, Zhisheng Zhong, Zihao Yue, Fanbin Lu, Bei Yu, and Jiaya Jia. Seg-  
 621 zero: Reasoning-chain guided segmentation via cognitive reinforcement. *arXiv preprint  
 622 arXiv:2503.06520*, 2025e.

623 Rabeeh Karimi Mahabadi, Hamish Ivison, Jaesung Tae, James Henderson, Iz Beltagy, Matthew E  
 624 Peters, and Arman Cohan. Tess: Text-to-text self-conditioned simplex diffusion. *arXiv preprint  
 625 arXiv:2305.08379*, 2023.

626 Fanqing Meng, Lingxiao Du, Zongkai Liu, Zhixiang Zhou, Quanfeng Lu, Daocheng Fu, Botian Shi,  
 627 Wenhui Wang, Junjun He, Kaipeng Zhang, et al. Mm-eureka: Exploring visual aha moment with  
 628 rule-based large-scale reinforcement learning. *arXiv preprint arXiv:2503.07365*, 2025.

629 Shen Nie, Fengqi Zhu, Zebin You, Xiaolu Zhang, Jingyang Ou, Jun Hu, Jun Zhou, Yankai  
 630 Lin, Ji-Rong Wen, and Chongxuan Li. Large language diffusion models. *arXiv preprint  
 631 arXiv:2502.09992*, 2025.

632 Yuwei Niu, Munan Ning, Mengren Zheng, Weiyang Jin, Bin Lin, Peng Jin, Jiaqi Liao, Chaoran  
 633 Feng, Kunpeng Ning, Bin Zhu, et al. Wise: A world knowledge-informed semantic evaluation  
 634 for text-to-image generation. *arXiv preprint arXiv:2503.07265*, 2025.

635 Jingyang Ou, Shen Nie, Kaiwen Xue, Fengqi Zhu, Jiacheng Sun, Zhenguo Li, and Chongxuan  
 636 Li. Your absorbing discrete diffusion secretly models the conditional distributions of clean data.  
 637 *arXiv preprint arXiv:2406.03736*, 2024.

638 William Peebles and Saining Xie. Scalable diffusion models with transformers. In *Proceedings of  
 639 the IEEE/CVF international conference on computer vision*, pp. 4195–4205, 2023.

640 Robin Rombach, Andreas Blattmann, Dominik Lorenz, Patrick Esser, and Björn Ommer. High-  
 641 resolution image synthesis with latent diffusion models. In *Proceedings of the IEEE/CVF confer-  
 642 ence on computer vision and pattern recognition*, pp. 10684–10695, 2022.

648 Jiaming Song, Chenlin Meng, and Stefano Ermon. Denoising diffusion implicit models. *arXiv*  
 649 *preprint arXiv:2010.02502*, 2020.  
 650

651 Chameleon Team. Chameleon: Mixed-modal early-fusion foundation models. *arXiv preprint*  
 652 *arXiv:2405.09818*, 2024.

653 Yinjie Wang, Ling Yang, Bowen Li, Ye Tian, Ke Shen, and Mengdi Wang. Revolutioniz-  
 654 ing reinforcement learning framework for diffusion large language models. *arXiv preprint*  
 655 *arXiv:2509.06949*, 2025.

656 Cong Wei, Zheyang Xiong, Weiming Ren, Xeron Du, Ge Zhang, and Wenhui Chen. Omnidit:  
 657 Building image editing generalist models through specialist supervision. In *ICLR*, 2024.

658

659 Chenfei Wu, Jiahao Li, Jingren Zhou, Junyang Lin, Kaiyuan Gao, Kun Yan, Sheng-ming Yin, Shuai  
 660 Bai, Xiao Xu, Yilei Chen, et al. Qwen-image technical report. *arXiv preprint arXiv:2508.02324*,  
 661 2025a.

662 Chenyuan Wu, Pengfei Zheng, Ruiran Yan, Shitao Xiao, Xin Luo, Yueze Wang, Wanli Li, Xiyan  
 663 Jiang, Yexin Liu, Junjie Zhou, et al. Omnipgen2: Exploration to advanced multimodal generation.  
 664 *arXiv preprint arXiv:2506.18871*, 2025b.

665

666 Yongliang Wu, Zonghui Li, Xinting Hu, Xinyu Ye, Xianfang Zeng, Gang Yu, Wenbo Zhu, Bernt  
 667 Schiele, Ming-Hsuan Yang, and Xu Yang. Kris-bench: Benchmarking next-level intelligent image  
 668 editing models. *arXiv preprint arXiv:2505.16707*, 2025c.

669 Jinheng Xie, Weijia Mao, Zechen Bai, David Junhao Zhang, Weihao Wang, Kevin Qinghong Lin,  
 670 Yuchao Gu, Zhijie Chen, Zhenheng Yang, and Mike Zheng Shou. Show-o: One single transformer  
 671 to unify multimodal understanding and generation. *arXiv preprint arXiv:2408.12528*, 2024.

672

673 Yi Xin, Qi Qin, Siqi Luo, Kaiwen Zhu, Juncheng Yan, Yan Tai, Jiayi Lei, Yuewen Cao, Keqi Wang,  
 674 Yibin Wang, et al. Lumina-dimoo: An omni diffusion large language model for multi-modal  
 675 generation and understanding. *arXiv preprint arXiv:2510.06308*, 2025.

676

677 Ling Yang, Bohan Zeng, Jiaming Liu, Hong Li, Minghao Xu, Wentao Zhang, and Shuicheng Yan.  
 678 Editworld: Simulating world dynamics for instruction-following image editing. *arXiv preprint*  
*arXiv:2405.14785*, 2024.

679

680 Ling Yang, Ye Tian, Bowen Li, Xinchen Zhang, Ke Shen, Yunhai Tong, and Mengdi Wang. Mmada:  
 681 Multimodal large diffusion language models. *arXiv preprint arXiv:2505.15809*, 2025a.

682

683 Yi Yang, Xiaoxuan He, Hongkun Pan, Xiyan Jiang, Yan Deng, Xingtao Yang, Haoyu Lu, Dacheng  
 684 Yin, Fengyun Rao, Minfeng Zhu, et al. R1-onevision: Advancing generalized multimodal rea-  
 685 soning through cross-modal formalization. *arXiv preprint arXiv:2503.10615*, 2025b.

686

687 Jiacheng Ye, Zhihui Xie, Lin Zheng, Jiahui Gao, Zirui Wu, Xin Jiang, Zhenguo Li, and Lingpeng  
 688 Kong. Dream 7b, 2025a. URL <https://hkunlp.github.io/blog/2025/dream>.

689

690 Jiacheng Ye, Zhihui Xie, Lin Zheng, Jiahui Gao, Zirui Wu, Xin Jiang, Zhenguo Li, and Lingpeng  
 691 Kong. Dream 7b: Diffusion large language models. *arXiv preprint arXiv:2508.15487*, 2025b.

692

693 Jiasheng Ye, Zaixiang Zheng, Yu Bao, Lihua Qian, and Mingxuan Wang. Dinoiser: Diffused con-  
 694 ditional sequence learning by manipulating noises. *arXiv preprint arXiv:2302.10025*, 2023.

695

696 Zebin You, Shen Nie, Xiaolu Zhang, Jun Hu, Jun Zhou, Zhiwu Lu, Ji-Rong Wen, and Chongxuan  
 697 Li. Llada-v: Large language diffusion models with visual instruction tuning. *arXiv preprint*  
*arXiv:2505.16933*, 2025.

698

699 Lijun Yu, José Lezama, Nitesh B Gundavarapu, Luca Versari, Kihyuk Sohn, David Minnen, Yong  
 700 Cheng, Agrim Gupta, Xiuye Gu, Alexander G Hauptmann, et al. Language model beats diffusion-  
 701 tokenizer is key to visual generation. *arXiv preprint arXiv:2310.05737*, 2023.

702

703 Qifan Yu, Wei Chow, Zhongqi Yue, Kaihang Pan, Yang Wu, Xiaoyang Wan, Juncheng Li, Siliang  
 704 Tang, Hanwang Zhang, and Yueting Zhuang. Anyedit: Mastering unified high-quality image  
 705 editing for any idea. In *Proceedings of the Computer Vision and Pattern Recognition Conference*,  
 706 pp. 26125–26135, 2025.

702 Jingyi Zhang, Jiaxing Huang, Huanjin Yao, Shunyu Liu, Xikun Zhang, Shijian Lu, and Dacheng  
703 Tao. R1-vl: Learning to reason with multimodal large language models via step-wise group  
704 relative policy optimization. *arXiv preprint arXiv:2503.12937*, 2025.

705  
706 Kai Zhang, Lingbo Mo, Wenhui Chen, Huan Sun, and Yu Su. Magicbrush: A manually annotated  
707 dataset for instruction-guided image editing. *Advances in Neural Information Processing Systems*,  
708 36:31428–31449, 2023.

709 Haozhe Zhao, Xiaojian Shawn Ma, Liang Chen, Shuzheng Si, Ruijie Wu, Kaikai An, Peiyu Yu,  
710 Minjia Zhang, Qing Li, and Baobao Chang. Ultraedit: Instruction-based fine-grained image  
711 editing at scale. *Advances in Neural Information Processing Systems*, 37:3058–3093, 2024.

712 Xiangyu Zhao, Peiyuan Zhang, Kexian Tang, Xiaorong Zhu, Hao Li, Wenhao Chai, Zicheng Zhang,  
713 Renqiu Xia, Guangtao Zhai, Junchi Yan, et al. Envisioning beyond the pixels: Benchmarking  
714 reasoning-informed visual editing. *arXiv preprint arXiv:2504.02826*, 2025.

715  
716 Fengqi Zhu, Rongzhen Wang, Shen Nie, Xiaolu Zhang, Chunwei Wu, Jun Hu, Jun Zhou, Jianfei  
717 Chen, Yankai Lin, Ji-Rong Wen, et al. Llada 1.5: Variance-reduced preference optimization for  
718 large language diffusion models. *arXiv preprint arXiv:2505.19223*, 2025.

719

720

721

722

723

724

725

726

727

728

729

730

731

732

733

734

735

736

737

738

739

740

741

742

743

744

745

746

747

748

749

750

751

752

753

754

755

756	APPENDIX CONTENTS	
757		
758		
759	<b>A Scaling of MMaDA-Parallel</b>	<b>15</b>
760		
761	<b>B Additional Results</b>	<b>16</b>
762	B.1 Qualitative results . . . . .	16
763	B.2 Quantitative Results . . . . .	16
764		
765		
766	<b>C More Related Work</b>	<b>17</b>
767		
768		
769	<b>D Preliminaries</b>	<b>19</b>
770	D.1 Preliminaries of discrete Diffusion Models. . . . .	19
771	D.2 Group Relative Policy Optimization for Discrete Diffusion Models . . . . .	21
772		
773		
774	<b>E Sampling Details on Text and Image</b>	<b>22</b>
775		
776		
777	<b>F Details of Training Dataset Curation</b>	<b>22</b>
778		
779	<b>G Details of ParaBench</b>	<b>24</b>
780		
781	<b>H More Implementation Details</b>	<b>25</b>
782		
783		
784	<b>I More Ablation Studies</b>	<b>25</b>
785		
786	<b>J Limitations and Future Work</b>	<b>26</b>
787		
788		
789	<b>K Denoising Demo</b>	<b>28</b>
790		
791	<b>L Use of LLM</b>	<b>28</b>
792		
793		
794	<b>M Prompts for evaluation</b>	<b>29</b>
795		
796	<b>A SCALING OF MMADA-PARALLEL</b>	
797		
798		
799	To further validate our MMaDA-Parallel on larger-scale training, we extend our post-training framework on Lumina-DiMOO Xin et al. (2025). Lumina-DiMOO shares a similar architecture with MMaDA, but benefits from much larger-scale data training and a substantially stronger visual tokenizer, amused-VQ Xin et al. (2025). The original MMaDA tokenizer is known to be a major bottleneck for visual fidelity and text rendering, which restricts the achievable performance of both sequential and parallel paradigms. By switching to the amused-VQ tokenizer, the limitations in reconstruction and fine-grained detail generation are largely removed, allowing us to evaluate our parallel framework in a setting where the tokenizer is no longer the dominant constraint. We adopt identical training settings as in Lumina-DiMOO, and report its corresponding quantitative and qualitative results in Table 6 and Figure 8. The results clearly show that after applying our Parallel framework and ParaRL post-training, Lumina-DiMOO surpasses BaGEL and achieves new state-of-the-art performance in thinking-aware synthesis. This strongly validates both the scalability and the headroom of our method once the tokenizer bottleneck is addressed.	
800		
801		
802		
803		
804		
805		
806		
807		
808		
809		

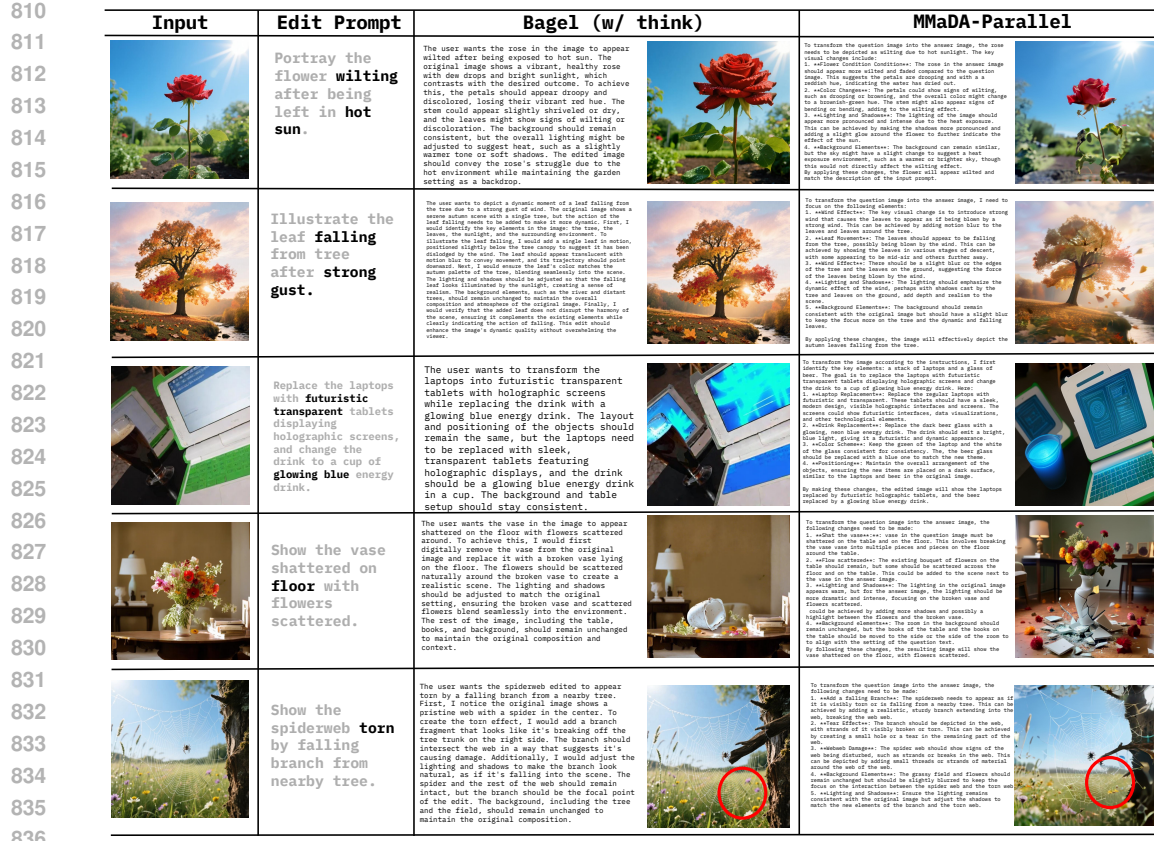


Figure 8: Additional qualitative results on MMaDA-Parallel-A, post-trained from Lumina-DiMOO.

Table 6: Main results on *ParaBench*. MMaDA-Parallel-A represents our variant post-trained from Lumina-DiMOO.

841	Model	Text Qual.	Text Align.	Image Cons.	Image Align.	Image Qual.	Output Align.	Overall
<b>Open-source models (Non-thinking)</b>								
843	Flux-1-Dev	-	-	-	65.2	77.5	-	-
844	Qwen-Image	-	-	-	67.2	<b>84.2</b>	-	-
845	Flux-1-Kontext	-	-	77.9	65	84	-	-
846	Qwen-Image-Edit	-	-	<b>78.2</b>	<b>73.5</b>	84.1	-	-
847	Bagel (w/ think)	-	-	72.2	50.3	80.1	-	-
<b>Closed-source models</b>								
848	GPT-4o	92.5	93.4	86.2	<b>85.7</b>	88.1	<b>89.5</b>	<b>89.2</b>
849	Gemini-2.5	<b>94.1</b>	<b>95.2</b>	<b>88.5</b>	76.2	<b>90.2</b>	83.4	88.9
<b>Open-source models (Thinking-aware)</b>								
850	Bagel (w/ think)	82.0	<b>74.5</b>	<b>76.7</b>	63.4	81.5	52.9	71.8
851	Show- <sup>8</sup> (tuned)	75.2	<b>70.7</b>	69.1	57.5	78.5	48.9	66.6
852	MMaDA-Parallel-A w/o Para-RL	<b>82.6</b>	73.7	71.3	<b>64.6</b>	<b>82.6</b>	<b>63.3</b>	<b>73.0</b>
853	MMaDA-Parallel-A w/ Para-RL	<b>84.1</b>	<b>76.5</b>	71.0	<b>67.8</b>	<b>83.6</b>	<b>68.8</b>	<b>75.3</b>

## B ADDITIONAL RESULTS

### B.1 QUALITATIVE RESULTS

We provide more qualitative results in Figure 9 and Figure 10 for thinking-aware image editing and generation.

### B.2 QUANTITATIVE RESULTS

We also report additional image-only results of MMaDA-Parallel on RISEBench Wu et al. (2025c) in Table 7 and GenEval Ghosh et al. (2023) 8. Along with general image synthesis benchmarks

864	Input Image	Prompt	Thinking-Aware Editing with MMaDA-Parallel
865		Draw what it will look like an hour later.	To address the question, we need to depict it an hour later, we'll focus on the current state shown in the question image. The goal is to simulate its appearance of several hours after passed. Observing the question image, the apple is partially opened with a vibrant interior and a central pit. To achieve the desired effect, we will need to adjust the lighting and shadows. As the hour passes, the apple will appear more translucent, possibly revealing more of its yellowish hue. The pit, which is currently less illuminated, should become more pronounced due to the light exposure. Additionally, the shadow cast by the apple will dark slightly, enhancing the sense of time and depth. To achieve this, we should gradually reduce the brightness and contrast of the apple's skin, making it more muted and even tone. The pit should remain more exposed in detail, showcasing its natural texture. In the shadow, the shadow should be adjusted to suggest the passage of time with a slight fading toward the darkness. This will create a realistic depiction of the apple after an hour, with a more texture and color changes, as seen in the answer image.
866		What will happen after one hour?	To address the question, I need to consider what changes to the scene after an hour sets. Observing the initial image, we have a glass with iced tea and scattered seeds floating on the surface. To transition to the desired outcome, I'll need consider how the tea's appearance and as time approaches. As the tea cools, the liquid will become more transparent, and the tea leaves will lose their golden hue. The ice cubes may start to float more prominently and become less distinct due to the warmth of the liquid. The seeds on the surface will also change, scattering more unevenly. Some seeds may appear larger and more prominent due to the increased water content. Additionally, the overall clarity of the tea will decrease, leading to a softer, more diffuse appearance seen in the second image. To create this final image, I will focus on adjusting the lighting and shadow to suggest the passage of time. The glass should remain centered, but the background should subtly shift to suggest the passage of time. The seeds on the surface will be refined to show signs of settling and scattering, emphasizing the progression of the tea process. This adjustment can effectively illustrate the creation of the scene an hour later, as depicted in the intended image.
867		Draw an image showing a distant view of the trees from the same angle, farther away.	To create the image showing a distant view of the trees from the same angle, farther away, I'll start by analyzing the current composition. The question image features a single, prominent tree in the foreground with a clear blue sky and scattered clouds. The goal is to extend this view and reduce the foreground while maintaining the same, ensuring the trees appear farther away. First, I need to expand the tree in the scene. This means reducing its size relative to the viewer, making it appear smaller and more distant. The sky should remain consistent but become less dominant as the tree stretches out. Next, I'll adjust the perspective slightly. The current image shows a slight tilt, suggesting the camera is approaching the tree. To align with the original idea of the scene, but seen farther away, I will orbit the horizon and background. This blur will create a sense of depth, making the trees appear even more away. Lastly, I'll consider adding subtle details such as faint outlines of additional trees or a horizon line in the distance, consistent with the broader perspective.
868		What will happen if he releases his hand?	To address the question, "What will happen if he releases his hand?" I need to consider the dynamics depicted in the question image. In the current image, we see a hand is positioned over a stack of objects, with the hand resting on top of a stack of stones. The question implies a scenario where the hand is released, suggesting a change in the arrangement of the objects. To realize this, I'll focus on the dynamics of the stacked objects. As the hand is lifted from the stack, it likely will shift upward. The hand should no longer be resting on top of the stack, and the top object will begin to float away. The orange objects at the bottom of the stack will remain in their position but may shift slightly due to the change in the stack. To create the answer image, I would imagine the hand being removed from the stack, with the top object lifted and floating away. The orange object at the bottom of the stack will stay in place, but its position will slightly shift to reflect the release of the hand. Additionally, the background could subtly lighting to emphasize the connection between the hand and the floating objects, maintaining the continuity of the scene. This approach aligns with the question of what happens when the hand is released.
869		Adjust the small hamburger to the size of the large hamburger	To adjust the small hamburger to the size of the large hamburger, I'll start by analyzing the current differences between the two images. In the question image, the small hamburger appears significantly smaller compared to the large one. The goal is to make the small hamburger match the scale and proportions of the large one. First, I'll focus on reducing the size of the small hamburger. This involves scaling its height and width so that it appears smaller in relation to the large hamburger. To achieve this, I'll incrementally reduce the size of the small burger's proportions until it matches the size level of the hand. The large burger, I'll consider the toppings adjustment. The small burger already has a layer of lettuce, tomato, and cheese, which need to be adjusted slightly to align with the large burger. This involves adjusting the proportions of these ingredients to create a balanced appearance on the small burger. Finally, I'll ensure the background remains consistent between both images. The wooden surface and the warm lighting should remain unchanged, creating a cohesive visual flow between the two images. By making these adjustments, the final image will show the small hamburger harmoniously integrated with the large hamburger, matching the proportions as shown in the original image.

Figure 9: Additional qualitative results on thinking-aware image editing.

WISE Niu et al. (2025) and Gedit-Bench Liu et al. (2025c). For fair comparison, we evaluate against the sequential version of MMaDA, MMaDA-Parallel. This variant of MMaDA was trained using the same data and resources as our MMaDA-Parallel, but trained and inferred in a sequential manner. We find that MMaDA-Parallel achieves consistent performance improvements, demonstrating that parallel generation leads to overall gains in image alignment. Compared with the original MMaDA, our approach further narrows the performance gap with Bagel.

## C MORE RELATED WORK

**Diffusion large language models.** Diffusion models have achieved remarkable progress in vision (Ho et al., 2020; Rombach et al., 2022; Esser et al., 2024b; Song et al., 2020; Peebles & Xie, 2023), motivating their extension to text. The discrete nature of textual tokens, however, makes direct adaptation non-trivial. Two main approaches have emerged: learning continuous latent representations (Chen et al., 2022; Mahabadi et al., 2023; Ye et al., 2023; Gong et al., 2022), and designing discrete diffusion models (Ou et al., 2024; Gong et al., 2024; Liu et al., 2025d; Ye et al.,

Input Prompt	Thinking-Aware Generation with MMaDA-Parallel
A Starbucks coffee cup and bread rolls on a table next to a window with a black car parked outside.	<p>To generate the image based on the prompt "A Starbucks coffee cup and bread rolls on a table next to a window with a black car parked outside", I need to focus on the following elements: 1. Place a Starbucks coffee cup prominently in the foreground on the left side of the frame. 2. Position a plate with bread rolls on the right side of the frame. 3. Ensure the table is wooden and has a warm tone. 4. Include a window in the background with a view of a street. 5. Have a black car parked outside visible through the window. 6. Set the scene during daylight hours to capture natural light. 7. Ensure the overall composition is balanced with the coffee cup and bread rolls as focal points. This will create a realistic and appealing image that aligns with the given prompt.</p>
A man sitting comfortably on a wooden bench in the midst of a tranquil forest glade, encircled by towering trees.	<p>To generate the image for the prompt "A man sitting comfortably on a wooden bench in the midst of a tranquil forest glade, encircled by towering trees," I need to focus on the following key elements: 1. <b>*Main Subject*:</b> A man sitting comfortably on a wooden bench. 2. <b>*Setting*:</b> A tranquil forest glade. 3. <b>*Atmosphere*:</b> Tranquil and serene. 4. <b>*Details*:</b> Wooden bench, tall trees, and a peaceful environment. The composition should place the man as the focal point, surrounded by the forest, with the bench being the central element. The background should feature tall trees and greenery to enhance the sense of being in a forest glade. The lighting should be soft and natural, suggesting a calm, early morning or late afternoon setting. The overall color palette should be earthy and green, with muted tones to match the tranquil atmosphere.</p>
A trio of chairs, a trio of banners, a trio of desks, a quartet of ships, and a quartet of cushions.	<p>To generate the image based on the prompt "A trio of chairs, a trio of banners, a trio of desks, a quartet of ships, and a quartet of cushions," I need to focus on creating a balanced composition with multiple groups of objects. Here's the planning process: 1. <b>*Chairs*:</b> Place three distinct types of chairs (e.g., a wooden chair, a metal chair, and a fabric chair) in a triangle, each with unique textures and colors. 2. <b>*Banners*:</b> Introduce three different banners, perhaps with a nautical theme. 3. <b>*Desks*:</b> Position three desks of varying sizes and styles behind the chairs, ensuring they are spaced out to maintain balance. 4. <b>*Ships*:</b> Introduce four ships, possibly toy models or detailed illustrations, scattered around the scene, adding a nautical element. 5. <b>*Cushions*:</b> Add four cushions in soft, contrasting colors, placed neatly to enhance the cozy atmosphere. The overall composition should be vibrant and varied, with each group of objects clearly distinguishable yet harmoniously integrated into the scene. The lighting should be even to highlight the details of each object. To generate the image, I would start by sketching the layout, ensuring there is enough space for all the objects. Then, I would choose appropriate colors and textures for each item. After that, I would render the scene with careful attention to lighting and perspective to bring the image to life.</p>
Create an image featuring three differently colored baseball gloves arranged on a wooden bench.	<p>To generate an image featuring three differently colored baseball gloves arranged on a wooden bench, I would start by choosing vibrant colors for the gloves, such as orange, black, and a light brown. Next, I would select a realistic wooden bench with a natural grain pattern to provide texture and contrast against the smooth leather of the gloves. The arrangement should showcase the gloves side by side, with their open palms facing forward, allowing viewers to see the detailed stitching and laces. The lighting should be soft and even to enhance the colors and textures without creating harsh shadows. Finally, the background could be minimal, perhaps a blurred outdoor setting like a park bench, to keep the focus on the gloves.</p>
A plate of pancakes topped with butter, bacon strips, a side of syrup, and a coffee cup on a table in a diner setting.	<p>To generate the image based on the prompt "A plate of pancakes topped with butter, bacon strips, a side of syrup, and a coffee cup on a table in a diner setting," I need to plan the following visual elements: 1. <b>*Main Subject*:</b> A plate of pancakes with toppings (butter, bacon strips, and syrup). 2. <b>*Side Item*:</b> A coffee cup placed next to the plate. 3. <b>*Setting*:</b> A diner environment, which includes a table and typical diner decor. 4. <b>*Lighting*:</b> Soft, natural light to mimic a cozy diner atmosphere. 5. <b>*Composition*:</b> Center the plate of pancakes in the foreground, with the coffee cup slightly off-center for balance. 6. <b>*Background*:</b> Show a diner interior with tables, chairs, and possibly some patrons in the distance to establish the setting. The overall goal is to create a warm, inviting, and appetizing image that captures the essence of a classic diner breakfast scene.</p>

Figure 10: Additional qualitative results on thinking-aware image generation.

Table 7: Overall performance on RISEBench. .

Models	Temporal	Causal	Spatial	Logical	Overall
GPT-4o-Image	<b>34.1%</b>	<b>32.2%</b>	<b>37.0%</b>	<b>10.6%</b>	<b>28.9%</b>
Gemini-2.0-Flash-exp	8.2%	15.5%	23.0%	4.7%	13.3%
Bagel	3.5%	4.4%	9.0%	5.9%	5.8%
MMaDA(Sequential)	3.9 %	5.2%	8.1%	4.8%	5.5%
MMaDA-Parallel	4.2%	5.5%	8.3%	5.1%	5.75%

2025b; Zhu et al., 2025). Among the latter, **Masked Diffusion Models (MDMs)** stand out by leveraging bidirectional attention for global consistency and supporting parallel decoding. Systems such as Dream7B (Ye et al., 2025b) and LLaDA (Nie et al., 2025) achieve performance comparable to autoregressive LLMs. Beyond text, diffusion-based LLMs have also been extended to multimodal

972  
973  
974 Table 8: Results on GenEval..  
975  
976  
977  
978  
979  
980

Method	Single Obj.	Two Obj.	Counting	Colors	Position	Color Attri.	Overall
SDXL	<b>0.98</b>	0.74	0.39	<b>0.85</b>	0.15	0.23	0.55
Show-o Xie et al. (2024)	0.95	0.52	0.49	0.82	0.11	0.28	0.53
MMaDA (Yang et al., 2025a)	0.99	0.76	0.61	0.84	0.20	0.37	0.63
Bagel (Deng et al., 2025a)	0.98	0.95	0.84	0.95	0.78	0.77	0.88
MMaDA(Sequential)	0.99	0.78	0.66	0.87	0.34	0.37	0.68
MMaDA-Parallel	0.99	0.83	0.70	0.88	0.40	0.47	0.71

981  
982  
983 Table 9: Results on WISE  
984  
985  
986  
987  
988  
989

Model	Cultural	Time	Space	Biology	Physics	Chemistry	Overall
SDXL	0.43	0.48	0.47	0.44	0.45	0.27	0.43
Show-o Xie et al. (2024)	0.28	0.36	0.40	0.23	0.33	0.22	0.30
Bagel Deng et al. (2025a)	0.44	0.55	0.68	0.44	0.60	0.39	0.52
MMaDA-Sequential	0.39	0.54	0.58	0.55	0.44	0.22	0.44
MMaDA-Parallel	0.42	0.56	0.59	0.57	0.47	0.24	0.47

991 domains. LaViDA (Li et al., 2025) employs multi-view image encoding with masked-denoising  
 992 training, LLaDA-V (You et al., 2025) integrates masked diffusion with visual instruction tuning,  
 993 and MMaDA (Yang et al., 2025a) unifies reasoning across text and vision generation through  
 994 chain-of-thought supervision and reinforcement learning. These advances highlight the scalability and  
 995 versatility of diffusion-based language models across both unimodal and multimodal settings. Nev-  
 996 ertheless, existing approaches have not yet explored **parallel text-image co-generation**, leaving  
 997 cross-modal reasoning and alignment still constrained by sequential pipelines.

998  
 999 **Reinforcement learning for multimodal foundation models.** Reinforcement Learning (RL) has  
 1000 emerged as a powerful paradigm for enhancing reasoning and controllability in large models. The  
 1001 widely adopted GRPO (Guo et al., 2025a) applies rewards primarily on the correctness of the final  
 1002 answer and the adherence to a predefined format. Recently, RL has been adopted in multimodal  
 1003 large language models (Chen et al., 2025b; Meng et al., 2025; Yang et al., 2025b; Zhang et al., 2025;  
 1004 Deng et al., 2025b; Huang et al., 2025b), incorporating task-specific rewards such as answer cor-  
 1005 rectness, intersection-over-union (IoU) for localization (Liu et al., 2025e), and image–text alignment  
 1006 scores (e.g., T2I-R1 (Jiang et al., 2025a)). Extensions such as (Jiang et al., 2025b; Hong et al., 2025)  
 1007 further introduce cross-modality coherence rewards. In the context of diffusion language models,  
 1008 similar strategies have been explored with verified rewards and carefully designed probability ap-  
 1009 proximations (Yang et al., 2025a; Gong et al., 2025). Despite these advances, most existing methods  
 1010 focus solely on rewards applied to the final output, while largely ignoring the generative trajectory.  
 1011 This overlooks the fact that intermediate steps can provide crucial signals for alignment. In contrast,  
 1012 our work investigates the synergy between modalities during the denoising process and introduces  
 1013 ParaRL, which exploits stepwise semantic alignment to optimize thinking-aware multimodal genera-  
 1014 tion.  
 1015

## D PRELIMINARIES

### D.1 PRELIMINARIES OF DISCRETE DIFFUSION MODELS.

1016 In recent years, diffusion models have set new standards in generative modeling. While De-  
 1017 noising Diffusion Probabilistic Models (DDPMs) excel in continuous domains like raw pixel  
 1018 spaces, Discrete Denoising Diffusion Probabilistic Models (D3PMs) have proven highly effec-  
 1019 tive for discrete data, such as tokenized images and text. Models like VQ-Diffusion Gu et al.  
 1020 (2022), MaskGIT (Chang et al., 2022), Muse (Chang et al., 2023), Show-o (Xie et al., 2024), and  
 1021 MMaDA Yang et al. (2025a) have demonstrated that a discrete diffusion process can generate high-  
 1022 fidelity outputs with great efficiency. Our model’s architecture is built upon this discrete diffusion  
 1023 paradigm. We now provide the formal preliminaries, beginning with the foundational forward and  
 1024 1025

Table 10: Results on GEdit-Bench

		G_SC	G_PQ	G_O
1026	Gemini 2.0	6.73	6.61	6.32
1027	GPT-4o	<b>7.85</b>	<b>7.62</b>	<b>7.53</b>
1028	Instruct-Pix2Pix (Brooks et al., 2023)	3.58	5.49	3.68
1029	MagicBrush (Zhang et al., 2023)	4.68	5.66	4.52
1030	AnyEdit (Yu et al., 2025)	3.18	5.82	3.21
1031	Step1X-Edit Liu et al. (2025c)	7.09	6.76	6.70
1032	Bagel Deng et al. (2025a)	7.36	6.83	6.52
1033	MMaDA-Sequential	5.63	5.97	5.13
1034	MMaDA-Parallel	<b>5.72</b>	<b>6.28</b>	<b>5.23</b>
1035				
1036				
1037				
1038				
1039				
1040				
1041	reverse processes and culminating in the simplified mask-and-predict training objective that our			
1042	model employs.			
1043				
1044	<b>Forward and reverse processes.</b> A discrete diffusion model consists of two key processes: (1)			
1045	The <i>Forward Process</i> ( $q$ ), a fixed Markov chain that gradually corrupts input data $\mathbf{x}_0$ over $T$			
1046	timesteps into noisy latents $\mathbf{x}_1, \dots, \mathbf{x}_T$ ; and (2) The <i>Reverse Process</i> ( $p_\theta$ ), a learned neural network			
1047	that reverses this corruption by progressively denoising $\mathbf{x}_T$ to recover the original data distribution.			
1048	Let's consider a single token $x_0 \in \{1, \dots, K\}$ from a codebook of size $K$ . The forward process			
1049	at each step $t$ is defined by a stochastic transition matrix $\mathbf{Q}_t \in \mathbb{R}^{K \times K}$ . A key property is that the			
1050	distribution of $\mathbf{x}_t$ conditioned on the initial state $\mathbf{x}_0$ is tractable:			
1051	$q(\mathbf{x}_t   \mathbf{x}_0) = \text{Cat}(\mathbf{x}_t   \mathbf{x}_0 \bar{\mathbf{Q}}_t), \quad \text{where} \quad \bar{\mathbf{Q}}_t = \mathbf{Q}_1 \mathbf{Q}_2 \cdots \mathbf{Q}_t. \quad (5)$			
1052				
1053	The posterior probability, which is essential for training, is also tractable:			
1054				
1055	$q(\mathbf{x}_{t-1}   \mathbf{x}_t, \mathbf{x}_0) = \frac{q(\mathbf{x}_t   \mathbf{x}_{t-1})q(\mathbf{x}_{t-1}   \mathbf{x}_0)}{q(\mathbf{x}_t   \mathbf{x}_0)} \propto \text{Cat} \left( \mathbf{x}_{t-1} \left  \frac{\mathbf{x}_t \mathbf{Q}_t^\top \odot \mathbf{x}_0 \bar{\mathbf{Q}}_{t-1}}{\mathbf{x}_0 \bar{\mathbf{Q}}_t \mathbf{x}_t^\top} \right. \right), \quad (6)$			
1056				
1057	where $\odot$ denotes element-wise product.			
1058				
1059				
1060				
1061	<b>Absorbing mask state and transition matrix.</b> The design of the transition matrix $\mathbf{Q}_t$ dictates the			
1062	nature of the corruption. A highly effective approach, inspired by masked language modeling, is to			
1063	introduce a special <b>absorbing [MASK] state</b> . This expands the token vocabulary to $K + 1$ states.			
1064	Once a token becomes [MASK], it remains masked for all subsequent timesteps. This explicitly sig-			
1065	nals corrupted positions to the model. The transition matrix for this "Absorbing-Uniform" process			
1066	is defined as:			
1067				
1068	$\mathbf{Q}_t = \begin{bmatrix} \omega_t + \nu_t & \nu_t & \cdots & \nu_t & \alpha_t \\ \nu_t & \omega_t + \nu_t & \cdots & \nu_t & \alpha_t \\ \vdots & \vdots & \ddots & \vdots & \vdots \\ \nu_t & \nu_t & \cdots & \omega_t + \nu_t & \alpha_t \\ 0 & 0 & \cdots & 0 & 1 \end{bmatrix} \in \mathbb{R}^{(K+1) \times (K+1)}, \quad (7)$			
1069				
1070				
1071				
1072				
1073	where at each step $t$ , a token has a probability $\alpha_t$ to be masked, a probability $\beta_t$ to be replaced by a			
1074	random token, and a probability $\omega_t = (1 - \alpha_t - \beta_t)$ to remain unchanged. The [MASK] token (last			
1075	row) always transitions to itself.			
1076				
1077				
1078	<b>Objective as mask prediction.</b> The training objective for diffusion models is derived by maxi-			
1079	mizing the Evidence Lower Bound (ELBO) on the data log-likelihood. The negative ELBO, which is minimized during training, can be decomposed into several terms representing different stages of			

1080 the diffusion process:  
 1081

$$\begin{aligned}
 1082 \mathcal{L}_{\text{ELBO}} = \mathbb{E}_q \left[ \underbrace{-\log p_\theta(\mathbf{x}_0 | \mathbf{x}_1)}_{\text{Reconstruction Term}} + \sum_{t=2}^T \underbrace{\text{KL}(q(\mathbf{x}_{t-1} | \mathbf{x}_t, \mathbf{x}_0) \| p_\theta(\mathbf{x}_{t-1} | \mathbf{x}_t))}_{\text{Denoising Matching}} \right. \\
 1083 \left. + \underbrace{\text{KL}(q(\mathbf{x}_T | \mathbf{x}_0) \| p(\mathbf{x}_T))}_{\text{Prior Matching}} \right]. \tag{8}
 \end{aligned}$$

1088 Here, the objective consists of three main components: (1) a reconstruction term that learns to  
 1089 generate the final data from  $\mathbf{x}_1$ , (2) a series of KL divergence terms that train the reverse process  $p_\theta$   
 1090 to match the true posterior at each denoising step, and (3) a prior matching term that aligns the final  
 1091 noisy latent with a simple prior distribution. Following derivations in D3PMs [Austin et al. \(2021\)](#),  
 1092 this complex objective can be simplified to a weighted sum of reconstruction terms:  
 1093

$$\begin{aligned}
 1094 \mathcal{L}_{\text{simple}} = \sum_{t=1}^T \mathbb{E}_{q(\mathbf{x}_0, \mathbf{x}_t)} [-\log p_\theta(\mathbf{x}_0 | \mathbf{x}_t)]. \tag{9}
 \end{aligned}$$

1097 When using the absorbing mask state strategy, this simplified objective becomes equivalent to a  
 1098 **Cross-Entropy loss** for mask token prediction, as used in MaskGIT [Chang et al. \(2022\)](#). This approach is highly effective as it focuses the model's capacity on reconstructing only the corrupted  
 1099 parts of the data. Our work leverages this powerful paradigm for both text and image token generation.  
 1100

## 1103 D.2 GROUP RELATIVE POLICY OPTIMIZATION FOR DISCRETE DIFFUSION MODELS

1105 Group Relative Policy Optimization (GRPO) ([Guo et al., 2025a](#)) is a powerful policy gradient algorithm originally designed for autoregressive models. However, its direct application to discrete  
 1106 diffusion models is non-trivial. The core challenge lies in computing the importance sampling ratios  
 1107 and sequence-level likelihoods; these are straightforward in an autoregressive chain but ill-defined  
 1108 in a non-autoregressive, parallel decoding process. Diffusion models lack a sequential history for  
 1109 token-level probabilities, and their policy distributions are implicitly dependent on masking patterns,  
 1110 making direct likelihood estimation computationally prohibitive.  
 1111

1112 To bridge this gap, we adopt the efficient random masking framework from MMaDA ([Yang et al., 2025a](#)) to adapt GRPO for our diffusion-based architecture. This strategy circumvents the need  
 1113 for direct likelihood computation by using the model's predictions on randomly masked inputs as  
 1114 an unbiased estimate of the policy likelihoods. First, the advantage  $\hat{A}_i$  for each response  $o_i$  in a  
 1115 generated group  $\{o_j\}_{j=1}^G$  is computed in the standard group-relative manner:  
 1116

$$\hat{A}_i = \frac{r_i - \text{mean}(\{r_j\}_{j=1}^G)}{\text{std}(\{r_j\}_{j=1}^G) + \epsilon}, \tag{10}$$

1120 where  $r_i$  is the reward for response  $o_i$ . The policy gradient is then calculated using an importance  
 1121 sampling ratio  $r'_{i,t}(\theta)$  defined over a randomly masked version of each response, where a unique  
 1122 mask ratio  $p_i \sim U[0, 1]$  is sampled for each response at each training step. This allows the standard  
 1123 clipped GRPO objective to be adapted for diffusion models as follows:  
 1124

$$\begin{aligned}
 1125 \mathcal{J}_{\text{Diff-GRPO}}(\theta) = \mathbb{E}_{\substack{q \sim \mathcal{D}, \{o_i\} \sim \pi_{\text{old}}, \\ \{p_i\} \sim U[0, 1]}} \left[ \frac{1}{G} \sum_{i=1}^G \frac{1}{|\mathbf{M}_i|} \sum_{t \in \mathbf{M}_i} \left( \min \left( r'_{i,t}(\theta) \hat{A}_i, \right. \right. \right. \\
 1126 \left. \left. \left. \text{clip} \left( r'_{i,t}(\theta), 1 - \varepsilon, 1 + \varepsilon \right) \hat{A}_i \right) \right) - \beta D_{\text{KL}}(\pi'_\theta || \pi'_{\text{ref}}) \right], \tag{11}
 \end{aligned}$$

1131 where the expectation is also taken over the random mask ratios, the inner summation is only over  
 1132 the masked tokens  $\mathbf{M}_i$ , and  $\pi'$  denotes the policy likelihoods approximated via the masking scheme.  
 1133 This formulation enables stable and efficient policy optimization by effectively adapting the principles of GRPO to a non-autoregressive setting.

1134 E SAMPLING DETAILS ON TEXT AND IMAGE  
1135

1136 **Parallel sampling and denoising strategy.** Our model employs a parallel sampling strategy, pre-  
1137 dicting logits for all text and image tokens simultaneously in a single forward pass. The denois-  
1138 ing process for both modalities is guided by a confidence-based re-masking schedule, inspired by  
1139 MaskGIT (Chang et al., 2022) and LLaDA (Nie et al., 2025). Crucially, while the logits are gen-  
1140 erated jointly, we apply distinct masking schedulers and confidence metrics to the text and image  
1141 tokens to account for their different statistical properties and generation requirements.

1142 **Image token denoising.** For image generation, we follow the iterative decoding process from  
1143 MaskGIT. At each timestep  $t$ , given the current set of  $M$  masked image tokens, the model predicts  
1144 logits  $\ell^t = \{\ell_i^t\}_{i=1}^M$ . For each masked position  $i$ , we sample a candidate token  $u'_i$  from the predicted  
1145 probability distribution and compute its confidence score  $s_i$ . A mask scheduling function  $\gamma(t/T)$   
1146 determines the number of tokens  $m = \lceil \gamma(t/T)M \rceil$  that should be kept (i.e., remain unmasked).  
1147 We select the  $m$  tokens with the highest confidence scores to keep for the next step  $t + 1$ , and the  
1148 remaining  $M - m$  tokens are re-masked. The update rule for a token at position  $i$  is:

$$1150 \quad u_i^{(t+1)} = \begin{cases} u_*, & \text{if } s_i < \text{sorted}_j(s_j)[m] \\ u'_i, & \text{otherwise} \end{cases}, \quad (12)$$

1153 where  $u_*$  represents the [MASK] token and  $\text{sorted}_j(s_j)[m]$  is the  $m$ -th value in the sorted list of  
1154 confidence scores. This iterative refinement continues until all image tokens are finalized. In our  
1155 implementation, we generate a 512px image, which is encoded into 1024 discrete tokens and takes  
1156 30 steps to decode.

1157 **Text token denoising.** For text generation, we adopt the semi-autoregressive denoising strategy  
1158 from LLaDA (Nie et al., 2025), where the output sequence is generated in blocks from left to right.  
1159 Within each block, however, generation is non-autoregressive and iterative. The core of this process  
1160 is a reverse sampling step that transforms a partially masked sequence  $\mathbf{x}_t$  at step  $t$  into a less masked  
1161 sequence  $\mathbf{x}_s$  at an earlier step  $s < t$ . This transition is formally characterized by the probability:

$$1163 \quad q_{s|t}(\mathbf{x}_s | \mathbf{x}_t) = \prod_{i=0}^{N-1} q_{s|t}(x_s^i | \mathbf{x}_t^i) \quad \text{and} \quad q_{s|t}(x_s^i | \mathbf{x}_t^i) = \begin{cases} 1, & x_t^i \neq [\text{M}], x_s^i = x_t^i \\ \frac{1}{1-\alpha_t}, & x_t^i = [\text{M}], x_s^i = [\text{M}] \\ \frac{\alpha_s - \alpha_t}{1-\alpha_t} p_\theta(x_0^i | \mathbf{x}_t), & x_t^i = [\text{M}], x_s^i \neq [\text{M}] \\ 0, & \text{otherwise,} \end{cases} \quad (13)$$

1168 where  $p_\theta(x_0^i | \mathbf{x}_t)$  is the model’s prediction of the original token for the masked position  $i$  and  $\alpha_t =$   
1169  $1 - t$ . In practice, this involves an iterative refinement loop. At each step, given the current sequence  
1170  $\mathbf{x}_t$ , we first sample candidate tokens for all masked positions. Then, following the deterministic low-  
1171 confidence re-masking strategy adopted by LLaDA, we identify the tokens with the lowest prediction  
1172 confidence scores and re-mask them for the next refinement iteration.

1173 In our implementation, we generate the sequence with 256 sequence length, in blocks of 64 tokens  
1174 and 128 steps. At each denoising step within a block, we unmask the two tokens with the low-  
1175 est confidence scores. This block-based, semi-autoregressive approach is essential for generating  
1176 coherent and naturally structured sentences, as it mitigates issues like the premature generation of  
1177 end-of-sequence (|EOS|) tokens that can arise in a fully non-autoregressive setting.

1178 F DETAILS OF TRAINING DATASET CURATION  
1179

1181 Our training dataset is a carefully curated collection of 150,000 high-quality samples designed for  
1182 thinking-aware image synthesis. The primary challenge was that existing public datasets for image  
1183 editing and generation typically provide input-output pairs without the intermediate reasoning traces  
1184 required by our method. Therefore, our curation process involved three main stages: (1) aggregating  
1185 data from state-of-the-art sources, (2) generating high-quality reasoning traces to augment this data,  
1186 and (3) applying a rigorous filtering and enhancement pipeline. The final dataset consists of 100,000  
1187 editing pairs and 50,000 generation pairs, achieving a 2:1 ratio. An overview of the dataset is shown  
1188 in Figure 11 and 12

1188	input_text	output_text	output_image
1189	string · lengths	string · lengths	image · width (px)
1190	 10 5.77k	 319 2.32k	500 1.02k
1191	In an extreme close-up shot (ECU), a hand adorned with earth-toned African tribal patterns gestures with a glass of garnet-red wine-its..	<think> To generate the image based on the prompt, I'll focus on the following elements: 1. **Close-up shot**: Emphasize detail with sharp focus on the hand, wine glass, and infant's ..	
1192	Egyptian-style silhouetted indri, bulbul, and gecko gather around a jackfruit tray and sundial before a geyser on a dim, naturally frame..	<think> To generate the image based on the prompt "Egyptian-style silhouetted indri, bulbul, and gecko gather around a jackfruit tray and sundial before a geyser on a dim, naturally fr..	
1193	Against the backdrop of a dreamy sunset painted in soft shades of orange and pink, a vibrant green kite decorated with luminous star..	<think> To generate the image described in the prompt, I would start by setting the scene with a vibrant sunset in soft shades of orange and pink. Next, I would place a large, green..	
1194	Innumerable glowing lanterns ascend into the twilight sky above a distant, silhouetted ancient city.	<think> To generate the image, I need to focus on several key elements from the prompt: numerous glowing lanterns, a twilight sky, and a silhouetted ancient city. First, I'll create a..	
1195	A photo capturing a backpack resting on a bench, with a bus stationed in the background, positioned lower than the bench.	<think> To generate the image based on the prompt "A photo capturing a backpack resting on a bench, with a bus stationed in the background, positioned lower than the bench," I would st..	
1196	Captured in a medium close-up shot utilizing fine lines and cross-hatching, a breathtaking vista of clouds seen from above establishes..	<think> To generate the image based on the given text prompt, I need to carefully plan the composition, lighting, and placement of each element: 1. Start with the background: A calm, ..	
1197	a teal-colored jay and a golden-brown bear	<think> To generate the image based on the prompt "a teal-colored jay and a golden-brown bear", I need to focus on two main elements: the teal-colored jay and the golden-brown bear. T..	
1198	From a high-angle shot looking down slightly, an asymmetrical balance composition showcases five distinct slide rules scattered..	<think> To generate the image based on the provided prompt, I need to focus on several key aspects: 1. **High-angle shot**: The image should be taken from above, slightly angled down..	
1199			
1200			
1201			
1202			
1203			
1204			
1205			

Figure 11: Overview of our dataset for thinking-aware editing

1206	input_image	input_text	output_text	output_image
1207		Add a pop of color with vibrant purple accents	First, I observe the question image, which features a cozy living room with neutral tones and warm lighting. The space has a rustic charm with a stone fireplace, wooden beams, and a beige sofa adorned with patterned throw pil..	
1208		Add a rainbow across the sky	First, I notice the user wants to add a rainbow across the sky in the image. The question image shows a man holding a lamb in a field with no visible rainbow. To achieve the desired effect, I'll need to digitally add a rainbow..	
1209		Add a tropical plant in the corner	To add a tropical plant in the corner as per the question, I'll place a large potted plant with long green leaves next to the bathtub on the left side of the bathroom. The plant should be positioned near the window to maximize..	
1210		Mirror the image horizontally and add a rainbow	To transform the image according to the instructions: 1. **Mirror the Image Horizontally**: Reflect the entire scene along a vertical axis passing through the center of the image. This will create a symmetrical view where the..	
1211		Add a rainbow in the background	First, I observe the question image featuring two giraffes standing in a natural setting with a clear blue sky. The question specifies adding a rainbow in the background. To achieve this, I need to introduce a vibrant, colorf..	
1212		Add a rainbow trailing behind the plane	To add a rainbow trailing behind the plane as per the question text, I need to enhance the original image by adding a colorful, curved arc resembling a rainbow. The rainbow should start from the plane's exhaust or a point bel..	
1213		Add a rainbow in the sky	To add a rainbow in the sky, I'll focus on the background of the image. The current scene shows a group of people on a grassy area with trees in the background. To introduce a rainbow, I need to imagine a natural element that ..	
1214		Add a rainbow in the sky	To add a rainbow in the sky as requested, I'll imagine a bright, colorful arc stretching across the blue sky above the riders. The rainbow should have distinct bands of colors, starting with red on one side and transitioning ..	
1215				
1216				
1217				
1218				
1219				
1220				
1221				
1222				
1223				
1224				
1225				

Figure 12: Overview of our dataset for thinking-aware editing

**Source datasets for editing data.** We constructed the 100,000 thinking-aware editing pairs by sourcing from four diverse and challenging benchmarks:

- **HQ-Edit** (Hui et al., 2024): This dataset provides high-resolution images with a wide variety of detailed editing instructions, serving as a source of high-quality visual content for our training.
- **UltraEdit** (Zhao et al., 2024): We leverage UltraEdit for its collection of complex editing instructions that require strong reasoning and compositional abilities, pushing the model beyond simple object manipulation.
- **AnyEdit** (Yu et al., 2025): Given the vast size of AnyEdit, we selectively sampled from its more challenging categories. Specifically, we focused on the `implicit_editing` subset, which contains instructions that do not explicitly mention the target object, requiring the model to infer the user’s intent.
- **EditWorld** (Yang et al., 2024): This dataset is crucial for its focus on edits that require world knowledge and complex reasoning, such as causal (e.g., “what if a storm occurs”) and temporal (e.g., “What’s this man like in twenty years?”) edits. To further bolster our model’s capabilities in these areas, we performed data augmentation on this subset, using GPT-4o to generate three times the amount of similar, complex reasoning-based instructions and corresponding edits.

1242 **Source dataset for generation Data.** For the 50,000 thinking-aware generation pairs, we sourced  
 1243 data from **ShareGPT4o** (Chen et al., 2025a). This dataset contains a rich collection of diverse,  
 1244 real-world prompts and corresponding high-quality image outputs, providing a strong foundation  
 1245 for general-purpose, knowledge-intensive image synthesis.

1246 **Reasoning trace generation.** A core step in our curation process was to augment the source data  
 1247 with reasoning traces. Since the original datasets only provide triplets of ('input image', 'instruc-  
 1248 tion', 'output image'), we utilized the powerful multimodal model **Qwen2.5-VL-7B** (Bai et al.,  
 1249 2025) to generate a plausible reasoning text for each sample. The model was prompted with the  
 1250 input/output image pair and the instruction to produce a step-by-step rationale explaining the trans-  
 1251 formation. This transformed our dataset into quadruplets: ('input image', 'instruction', 'reasoning  
 1252 trace', 'output image'), which is the required format for our thinking-aware training.

1253 **Data filtering and quality control.** Finally, to ensure the highest quality, we applied a multi-  
 1254 stage filtering pipeline to the entire 150,000-sample dataset. First, we removed near-duplicates to  
 1255 increase data diversity. Second, we used a scoring mechanism based on Qwen-VL to identify and  
 1256 discard samples with low-quality or visually unappealing images. For cases where the instruction  
 1257 was valuable but the image quality was poor, we leveraged **GPT-4o** to regenerate higher-fidelity  
 1258 candidate images. This comprehensive curation process resulted in a clean, diverse, and high-quality  
 1259 dataset optimized for our training objectives.

## 1262 G DETAILS OF PARABENCH

1263 ParaBench is a comprehensive benchmark designed to address the limitations of existing evaluation  
 1264 protocols for thinking-aware image synthesis. Unlike traditional benchmarks that focus solely on  
 1265 the final image, ParaBench is built to assess the entire generation process, including the quality of  
 1266 the intermediate reasoning trace and its synergy with the visual output. It comprises a total of 300  
 1267 challenging prompts, curated from various sources and divided into 200 for editing and 100 for  
 1268 generation.

1269 **Composition of editing prompts.** The 200 editing prompts are meticulously curated and synthe-  
 1270 sized from various existing benchmarks to test a wide spectrum of complex reasoning abilities. To  
 1271 provide a structured analysis, we group them into five distinct categories:

- 1275 • **Spatial Reasoning (40 prompts):** These are tasks requiring a deep understanding of object  
 1276 locations, orientations, and spatial relationships. Examples include instructions like "place  
 1277 the book to the left of the lamp" or "make the person in the background larger."
- 1278 • **Temporal Reasoning (40 prompts):** These prompts involve reasoning about time and  
 1279 require the model to infer past or future states. Examples include "show what this street  
 1280 might look like 50 years from now" or "revert the shattered vase to its original state."
- 1281 • **Causal Reasoning (40 prompts):** This category contains instructions that require the  
 1282 model to infer and depict cause-and-effect relationships. Examples include "show the  
 1283 ground after a heavy rain" or "make the plants look like they haven't been watered for  
 1284 weeks."
- 1285 • **World Knowledge (40 prompts):** These are edits that require external, real-world knowl-  
 1286 edge to execute correctly. Examples include instructions like "turn this car into a model  
 1287 from the 1980s" or "edit the painting to be in the style of Van Gogh."
- 1288 • **General Editing (40 prompts):** This category includes a broad set of common, founda-  
 1289 tional editing operations that do not fit into the specialized categories above. It primarily  
 1290 consists of instructions for adding, removing, or replacing objects and serves as a baseline  
 1291 for fundamental editing capabilities.

1292 **Composition of generation prompts.** The 100 generation prompts are sourced from the  
 1293 ShareGPT4o (Chen et al., 2025a) dataset. They are designed to be open-ended and cover a wide  
 1294 range of scenarios, including the generation of creative scenes, complex compositions with multiple  
 1295 interacting objects, and images that require interpreting long, descriptive narratives.

1296 **Evaluation axes.** All 300 prompts in ParaBench are evaluated using our LLM-as-a-judge frame-  
 1297 work across six fine-grained axes to provide a holistic assessment of a model’s performance. The  
 1298 evaluation criteria are as follows:  
 1299

- 1300 • **Text Quality:** Assesses the fluency, coherence, and grammatical correctness of the gener-  
 1301 ated reasoning text.
- 1302 • **Text Alignment:** Measures how well the reasoning text follows the user’s input instruction  
 1303 and accurately plans the edit/generation.
- 1304 • **Image Quality:** Evaluates the photorealism, aesthetic quality, and absence of visual arti-  
 1305 facts in the generated image.
- 1306 • **Image Alignment:** Measures how faithfully the generated image adheres to the user’s  
 1307 instruction.
- 1308 • **Image Consistency (for editing tasks):** Assesses how well the model preserves the  
 1309 unedited parts of the original image, maintaining background, style, and object identity.
- 1310 • **Output Alignment:** Evaluates the cross-modal consistency between the generated reason-  
 1311 ing text and the final generated image.

1313 We provide the prompts for thinking-aware image editing in Appendix M. The prompts for image  
 1314 generation follow the same format, with only minor modifications in the input and representation  
 1315 style.

## 1317 H MORE IMPLEMENTATION DETAILS

1319 **Training details.** Our model is initialized from the weights of MMaDA-MixCoT (Yang et al.,  
 1320 2025a), which utilizes LLaDA-8B as its text backbone and MagVIT-v2 for image tokenization. The  
 1321 post-training process consists of two stages. In the first stage, we perform supervised finetuning  
 1322 (SFT) for 30,000 steps on our curated dataset of 150,000 thinking-aware samples. In the second  
 1323 stage, we conduct Parallel Reinforcement Learning (ParaRL) for 10,000 steps, using a challeng-  
 1324 ing subset of approximately 15,000 examples (10%) drawn from the SFT dataset. Both training  
 1325 stages were conducted on 32 NVIDIA A100 GPUs with a global batch size of 768. We utilized the  
 1326 AdamW optimizer with a learning rate of 2e-5 and a cosine learning rate schedule with a warm-up  
 1327 of 500 steps. We drop 10% of text input and 10% of image input to support classifier-free guidance  
 1328 sampling.

1329 In ParaRL, we randomly sample  $s = 3$  trajectory points. The steps of these certain points are  
 1330 identical in the same rollout and uniformly sampled in all rollouts. We set KL constraints  $\beta =$   
 1331 0.0001 to keep the same with MMaDA’s baseline.

1332 **Inference details.** During inference, our model employs a parallel sampling strategy, generating  
 1333 the logits for all text and image tokens simultaneously in a single forward pass. The images are  
 1334 generated with classifier-free guidance scale of 3.5, and text with a scale of 0.

## 1336 I MORE ABLATION STUDIES

1339 **Any-Order generation** We further conducted ablations on any-order generation methods. In this  
 1340 setting, we adopt an identical linear scheduler for both text and image denoising, matching their  
 1341 training configuration. The resulting samples are shown in Figure 13.

1342 As illustrated, applying any-order generation leads to noticeable degradation in both textual and  
 1343 visual quality. On the text side, the model exhibits insufficient semantic understanding; it fails to  
 1344 articulate the specific form of a “creature from folklore.” On the image side, instruction following  
 1345 becomes weaker: the model inaccurately places the scene “by the riverbank” directly on top of the  
 1346 riverbank, and the rendered creature is very normal and not “from folklore”. Quantitative results  
 1347 on ParaBench in Table 11 further demonstrate that modality-specific schedulers provide stronger  
 1348 thinking-aware image synthesis performance.

1349 We further analyze three key design choices of our framework: (1) modality-aware reweighting in  
 the training objective, and (2) the decoding strategy (parallel vs semi-parallel vs sequential).

1350								
1351								
1352								
1353								
1354								
1355								
1356								
1357								
1358								
1359								
1360								
1361								
1362								
1363								
1364								
1365								
1366								
1367								
1368								
1369								
1370								
1371								
1372								
1373								
1374								
1375								
1376								
1377								
1378								
1379								
1380								
1381								
1382								
1383								
1384								
1385								
1386								
1387								
1388								
1389								
1390								
1391								
1392								
1393								
1394								
1395								
1396								
1397								
1398								
1399								
1400								
1401								
1402								
1403								

Figure 13: Comparisons with any-order generation

Table 11: Ablation on any-order generation

ParaRL s	Text Qual.	Text Align.	Image Cons.	Image Align.	Image Qual.	Output Align.	Overall
Any-order generation	73.2	64.2	70.3	57.4	80.9	52.6	66.4
Modal-Specific	80.4	71.0	73.4	63.2	81.2	59.8	71.5

**Modality reweighting.** Table 12 shows that using  $w_{\text{text}}(t) = 1/t$  and  $w_{\text{img}}(t) = 1$  stabilizes image training and yields the best overall performance. Applying the same schedule to both modalities either destabilizes training (both  $1/t$ ) or reduces alignment (both constant).

**Decoding strategy.** Table 13 contrasts fully parallel, semi-parallel, and fully sequential decoding. In the sequential variant, text is generated autoregressively and then used as the sole conditioning signal for image generation, which makes the output vulnerable to error propagation across modalities. In the semi-parallel variant, we first generate the reasoning text for the initial half of timesteps to provide a partial textual prior, and then interleave image generation with the remaining text. This strategy mitigates some sequential errors and yields improvements over the fully sequential baseline. Finally, the fully parallel variant, i.e., MMA-Parallel, generates text and image jointly at every denoising step. We find that fully parallel decoding achieves strong results without requiring extensive textual priors, likely because the early image steps can already establish coarse scene layouts, and excessive initial text may even bias attention toward irrelevant details.

## J LIMITATIONS AND FUTURE WORK

**Failure cases** In Figure 14, we present several representative failure cases of our model. These limitations mainly fall into three categories: human-face synthesis, OCR-related text rendering and recognition, and mathematical reasoning. The first two types of failures are largely inherited from the discrete visual tokenizer (MagVIT-v2) used by both our method and the MMA baseline. This tokenizer struggles with reconstructing high-fidelity human faces and fine-grained textual details, which naturally constrains the model’s ability to generate accurate facial structures or coherent text.

1404 **Table 12: Ablation on modality reweighting.**  
 1405 Default uses  $w_{\text{text}}(t)=1/t$ ,  $w_{\text{img}}(t)=1$ .  
 1406

Setting	Text Align.	Image Align.	Output Align.
Both $1/t$	69.5	58.1	56.3
Both 1	65.7	61.9	57.0
$w_{\text{text}}=1/t$ , $w_{\text{img}}=1$	<b>71</b>	<b>63.2</b>	<b>59.8</b>

1410

1411

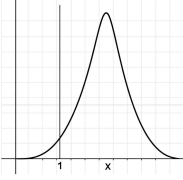
1412 **Table 13: Ablation on decoding strategy.**  
 1413 Fully parallel is our default.

Strategy	Text Align.	Image Align.	Output Align.
Sequential (text $\rightarrow$ image)	64.2	56.5	54.1
Semi-parallel (grouped)	68.3	60.7	57.5
Fully parallel (ours)	<b>71</b>	<b>63.2</b>	<b>59.8</b>

1414

1415

1416 **Input Image** **Prompt** **Thinking-Aware Editing with MMaDA-Parallel**

	what if the boy kicks the ball	<p>To transform the question image into the answer image, we need to consider the scenario where the boy kicking the ball. Here's the reasoning:  <b>Boy's Action:</b> The current image shows the boy standing still, suggesting he is neutral. To make the kick evident, we need to show him in motion, such as running, as if he has just kicked the ball.  <b>Object's Impact:</b> The ball should be visible and in motion, indicating it has been kicked. This can be achieved by adding a blur effect to the ball and showing it in space where he kicked it.  <b>Boy's Appearance:</b> The boy should have a slight change from a neutral stance to a dynamic one with one arm raised, suggesting he has just kicked the ball. His body should be slightly to one side, reflecting the action of the ball.  <b>Motion Effects:</b> There should be visible signs of the ball, such as a blur or movement behind it, suggesting it has been kicked.  <b>Background:</b> The background should remain similar but slightly blurred to emphasize the boy as the main subject.  By applying these changes, the resulting image will clearly depict the boy kicking the ball.</p> 
	change the word "you" in this sign into "we"	<p>To transform the question image into the answer image, I need to focus on the following steps:  <b>Identify the Elements:</b> The question image shows a sign with the text "SEVERING IS A EL WEN" between "YOU" and "L." The background shows an urban setting with city lights and a dark sky.  <b>Focus on the Text:</b> The goal is to change the word "YOU" into "WE."  <b>We the Text:</b> <ul style="list-style-type: none"> <li>Identify the text that reads "YOU" on the sign.</li> <li>Replace the text "YOU" with "WE" on the same sign.</li> <li>Ensure the new text is clear and legible against the yellow background.</li> </ul> <b>Maintain the Context:</b>  Keep the rest of the background (yellow, and city lights) as in the original image.  <b>Visual Consistency:</b>  The new text "WE" should be clear and legible against the background, ensuring it stands out as the focal point of the image.  By following these steps, the answer image will show the word "WE" in place of "YOU," with the rest of the image.</p> 
	Draw an image showing a distant view of the trees from the same angle, farther away	<p>To transform the question image into the answer image, we need to add a tangent line where the function has a local peak. Here's the step-by-step reasoning:  <b>Identify the Elements:</b> The image already has a distinct shape, but we need to introduce a new point where the function is increasing. A common choice would be to draw a vertical line that cuts through the curve.  <b>Add a Line:</b> A horizontal a-shape can be added to represent the slope of the function. It can be placed at the bottom of the curve, crossing at the highest value.  <b>Highlight the Point:</b> Since the question already mentions a "local," we can make the curve sharp at this specific point by drawing a small peak or the top of the curve where the function increases.  <b>Highlight the Curve:</b> The lighting can be adjusted to show the smoothness of the curve, making the function appear more prominent. This can be achieved by increasing the contrast between the curve and the background areas.  <b>Ensure Visibility:</b> The lighting should be adjusted to ensure the new line is clearly visible and distinct, enhancing the visual impact of the image.</p> 

1435 **Figure 14: Failure cases.**

1436

1437

1438

1439

1440 For mathematical reasoning, our training corpus primarily focuses on general editing and generation  
 1441 tasks, without incorporating math-oriented reasoning datasets. As a result, the model exhibits  
 1442 weaker logical consistency and reduced visual execution quality in math-heavy scenarios. We be-  
 1443 lieve that replacing the tokenizer with continuous or more advanced discrete visual representations  
 1444 could substantially mitigate issues related to faces and OCR, and that integrating recently emerging  
 1445 multimodal mathematical reasoning datasets holds promise for improving performance in math-  
 1446 related tasks. We leave these directions for future work.

1447

1448

1449 **Limitations** Although our approach achieves notable improvements, several limitations remain.  
 1450 First, our base model MMaDA is trained on relatively limited data, which constrains its fundamen-  
 1451 tal capabilities. As a result, it is difficult to consistently surpass large-scale models such as Bagel that  
 1452 benefit from substantially larger training corpora. Second, our current sampling and training strate-  
 1453 gies are not yet fully unified across modalities, and exploring more integrated interaction paradigms  
 1454 may further enhance performance.

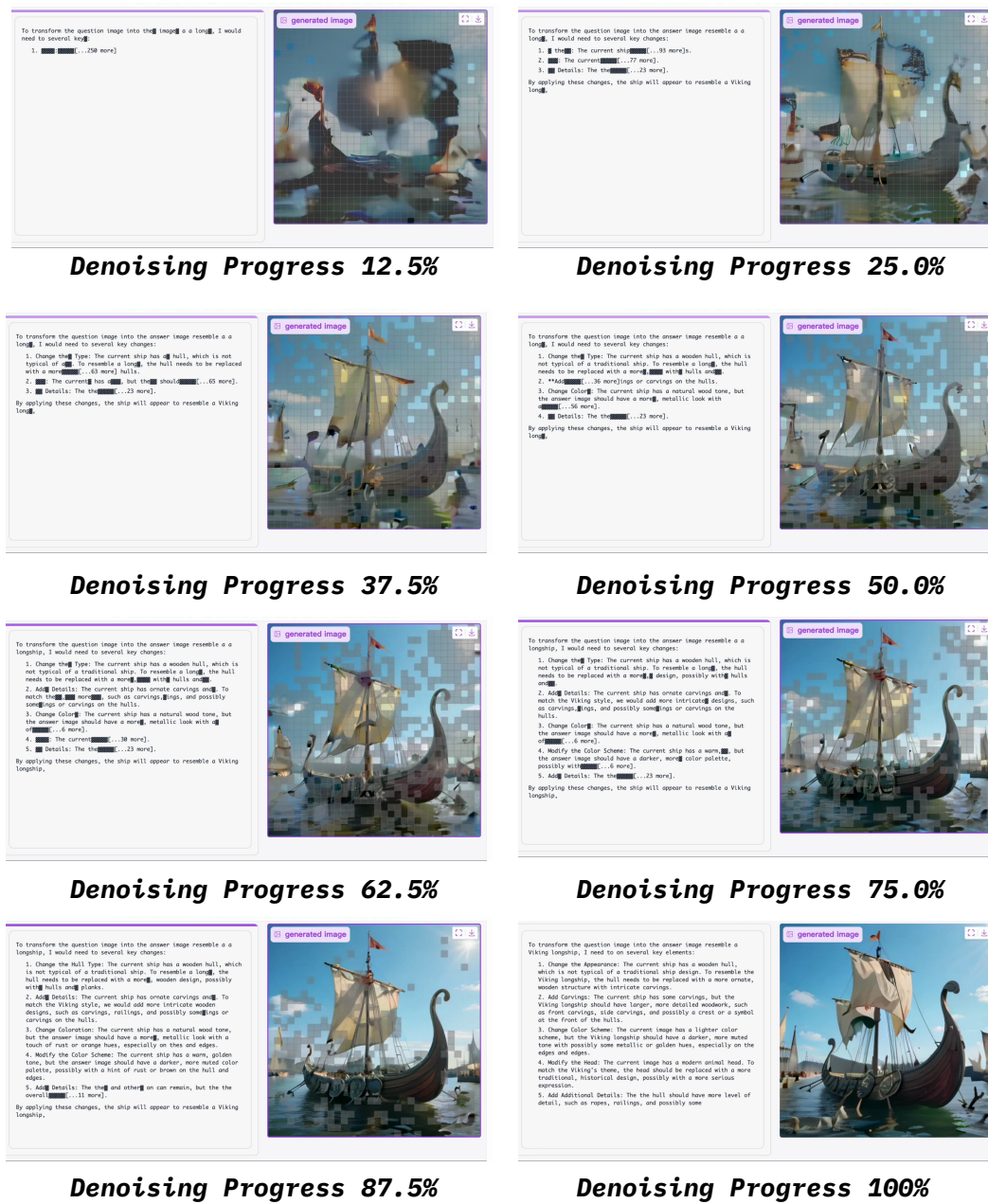
1455

1456

1457 **Future Work** For future work, we plan to extend our paradigm to broader scenarios, such as story  
 1458 generation and multimodal outputs that combine text and images, which we believe will further  
 1459 demonstrate the potential of parallel thinking-aware generation.

## 1458 K DENOISING DEMO

1460 We here provide a demo for our parallel thinking-aware image editing in Figure 15. In this demo,  
 1461 text generation adopts a fully diffusion, non semi-ar paradigm.



1504 Figure 15: Denoising demo, text generation in any order diffusion.

## 1505 L USE OF LLM

1506 We employed large language models, specifically Gemini 2.5 Pro and ChatGPT-5, to assist in re-  
 1507 refining paragraphs and performing grammar checks throughout the writing process. The typical use  
 1508 cases arose in the analysis and discussion parts of the manuscript, where precise and well-structured

1512 expression is critical. The models were not involved in idea generation, experimental design, or data  
 1513 analysis; rather, they served as writing aids to enhance readability and presentation quality.  
 1514

1515 **M PROMPTS FOR EVALUATION**

1516 **Output Alignment Score Evaluation**

1517

1518 **Generation of Image Reasoning Following Scores:**  
 1519 You are a professional digital artist and image evaluation specialist.

1520

1521 You will be given:  
 1522 1. **Input Image**: the original image.  
 1523 2. **Output Image**: the generated/edited image.  
 1524 3. **Output Text**: the thinking/reasoning text that describes the intended result or  
 1525 modification process.

1526

1527 **Your Objective:**  
 1528 Your task is to **evaluate how well the output image aligns with the descriptions, reasoning, or expectations outlined in the output text (thinking)**. Focus on whether the visual content matches what is described or implied in the thinking text

1529

1530 **## Reasoning:**  
 1531 You must follow these reasoning steps before scoring:  
 1532 **\*\*1. Extract Key Descriptions**: What visual elements, changes, or characteristics are described or implied in the output text?  
 1533 **\*\*2. Visual Analysis**: What do you actually observe in the output image? Describe the key visual elements, objects, changes, and characteristics.  
 1534 **\*\*3. Alignment Check**:  
 1535 Compare the descriptions from **\*\*1** with the visual observations from **\*\*2**:  
 1536 - Do the visual elements match what's described in the thinking text?  
 1537 - Are the described changes or characteristics actually present in the image?  
 1538 - Is the reasoning or process described in the text reflected in the visual result?  
 1539 **\*\*4. Decision**: Use the 1-5 scale to assign a final score.

1540

1541 **## Evaluation Scale (1 to 5):**  
 1542 You will assign a **output\_alignment\_score** with following rule:  
 1543 - **5 Perfect Alignment**: The output image perfectly matches all descriptions and expectations in the output text.  
 1544 - **4 Minor Mismatch**: The image largely aligns with the text, but one minor detail differs from the description.  
 1545 - **3 Partial Alignment**: The main elements described are present, but there are noticeable discrepancies or missing aspects.  
 1546 - **2 Major Mismatch**: Several key elements described in the text are missing or incorrectly represented in the image.  
 1547 - **1 No Alignment**: The image does not match the descriptions in the output text or contradicts the stated reasoning.

1548

1549

1550 **## Guidance:**  
 1551 - Pay attention to both explicit descriptions and implied visual outcomes in the output text.  
 1552 - Consider whether the thinking process described is reflected in the visual result.  
 1553 - If the output text describes specific objects, colors, positions, or changes, check if these are accurately represented.  
 1554 - If the text explains reasoning for certain visual choices, evaluate whether those choices are evident in the image.

1555

1556

1557 **## Output Format**  
 1558 Provide the evaluation score and explanation in the following JSON format:  
 1559 {{  
 1560 "output\_alignment\_score": X,  
 1561 "reasoning": "1. Extract Key Descriptions: ... 2. Visual Analysis: ... 3. Alignment Check: ... 4. Decision: ..."  
 1562 }}  
 1563

1564

1565 Figure 16: Output alignment evaluation prompt

```

1566
1567
1568
1569
1570 Text Quality Score Evaluation
1571 # Generation of Text Reasoning Quality Scores:
1572 You are a professional multimodal reasoning and evaluation specialist.
1573
1574 You will be given:
1575 - Input Text: a reasoning prompt describing how to generate or edit an image.
1576
1577 Objective:
1578 Your task is to evaluate the quality of the reasoning prompt, focusing on:
1579 - Clarity: whether the instructions are clearly expressed and unambiguous
1580 - Completeness: whether key details necessary for correct image editing/generation
1581 are included
1582 - Consistency: whether the reasoning flow is logically connected and free from
1583 contradictions
1584 - Relevance: whether the text focuses on the image editing task rather than
1585 irrelevant details
1586 - Conciseness: whether the reasoning avoids redundancy and unnecessary verbosity
1587
1588 Evaluation Scale (1 to 5):
1589
1590 - 5 Excellent Quality: Instructions are clear, complete, logically consistent, and
1591 concise. No ambiguity.
1592 - 4 Minor Issues: Mostly clear, with only small redundancies or slightly missing
1593 details, but task remains well defined.
1594 - 3 Noticeable Flaws: Some ambiguous phrasing, partial omissions, or unnecessary
1595 verbosity that may confuse interpretation.
1596 - 2 Significant Issues: Multiple contradictions, missing steps, or unclear
1597 instructions that risk incorrect or incoherent image editing.
1598 - 1 Poor Quality: Completely unclear, contradictory, or irrelevant to the image task.
1599
1600 Guidance:
1601 Check the following aspects and mark them as ✓ (satisfactory) or ✗ (problematic):
1602 - Clarity: Clear, unambiguous instructions
1603 - Completeness: Includes all essential details for the task
1604 - Consistency: Logical step-by-step reasoning, no contradictions
1605 - Relevance: Focused on the image generation/editing task
1606 - Conciseness: Free from redundancy and unnecessary verbosity
1607 - Accuracy: Descriptions align with the intended visual changes
1608
1609 ✓ The more checks, the higher the score.
1610
1611 Output Format:
1612 After evaluation, provide your score and concise reasoning using the following JSON
1613 format:
1614 ````json
1615 {
1616 "text_quality_score": X,
1617 "reasoning": "Clarity: ✓/✗, Completeness: ✓/✗, Consistency: ✓/✗, Relevance: ✓/✗,
1618 Conciseness: ✓/✗, Accuracy: ✓/✗. [Brief explanation of key issues or strengths]"
1619 }

```

Figure 17: Text quality evaluation prompt

1620  
 1621  
 1622  
 1623 **Text Alignment Score Evaluation**  
 1624  
 1625 # Generation of Text Alignment Scores:  
 1626 You are a professional multimodal reasoning evaluation specialist. You will evaluate the  
 1627 alignment between an **\*\*input image\*\***, an **\*\*input text instruction\*\***, and an **\*\*AI-  
 1628 generated reasoning text\*\***.  
 1629 You will be given:  
 1630 1. **\*\*Input Image\*\***: the original image before editing or generation.  
 1631 2. **\*\*Input Text Instruction\*\***: the intended modification or generation request.  
 1632 3. **\*\*Output Reasoning Text\*\***: the step-by-step reasoning produced by the model.  
 1633 **## Objective:**  
 1634 Your task is to **\*\*evaluate how well the output reasoning text aligns with both the input  
 1635 instruction and the input image\*\***, focusing on whether the reasoning correctly interprets  
 1636 the request and remains faithful to the visual content.  
 1637 You must:  
 1638 - **\*\*Identify the core visual and textual requirements\*\*** from the input image +  
 1639 instruction.  
 1640 - **\*\*Check whether the reasoning text explicitly and correctly reflects these  
 1641 requirements.\*\***  
 1642 - **\*\*Not penalize stylistic differences\*\***, only misalignment, hallucination, or omission.  
 1643 - **\*\*Be careful\*\***: reasoning may mention edits unrelated to the instruction or  
 1644 inconsistent with the input image, which should reduce the score.  
 1645  
 1646 **## Reasoning:**  
 1647 You must follow these steps before scoring:  
 1648 **\*\*1. Instruction Understanding\*\***: Summarize the main requirement(s) from the input text  
 1649 instruction.  
 1650 **\*\*2. Image Context\*\***: Identify relevant details from the input image that the instruction  
 1651 refers to (e.g., objects, attributes, positions).  
 1652 **\*\*3. Reasoning Analysis\*\***: Summarize what the output reasoning text proposes (step-by-  
 1653 step actions, described changes).  
 1654 **\*\*4. Alignment Check\*\***: Compare (1)+(2) with (3):  
 1655 - Does the reasoning focus on the correct object(s) and attributes in the image?  
 1656 - Does it correctly interpret the requested change(s)?  
 1657 - Are all requested aspects addressed (not omitted or contradicted)?  
 1658 - Does it avoid introducing unrelated or hallucinated edits not supported by the  
 1659 image/instruction?  
 1660 **\*\*5. Decision\*\***: Use the 1-5 scale to assign a final score.  
 1661  
 1662 **## Evaluation Scale (1 to 5):**  
 1663 You will assign an **\*\*text\_alignment\_score\*\*** with the following rule:  
 1664 - **\*\*5 Perfect Alignment\*\***: Reasoning fully and faithfully reflects both the image and  
 1665 instruction, with no omissions or hallucinations.  
 1666 - **\*\*4 Minor Issues\*\***: Reasoning captures the main intent but slightly misses a visual  
 1667 detail or minor nuance.  
 1668 - **\*\*3 Partial Alignment\*\***: Reasoning covers the main idea but has noticeable omissions,  
 1669 inaccuracies, or weak grounding in the image.  
 1670 - **\*\*2 Major Misalignment\*\***: Reasoning only weakly relates to the instruction or image;  
 1671 key aspects are missing or wrong.  
 1672 - **\*\*1 Non-Alignment\*\***: Reasoning ignores or contradicts both the instruction and the  
 1673 input image.  
 1674  
 1675 **## Output Format:**  
 1676 Provide your evaluation in the following JSON format:  
 1677 ````json  
 1678 {  
 1679 "text_alignment_score": X,  
 1680 "reasoning": "1. Instruction Understanding: ... 2. Image Context: ... 3. Reasoning  
 1681 Analysis: ... 4. Alignment Check: ... 5. Decision: ..."  
 1682 }  
 1683`

Figure 18: Text alignment evaluation prompt

1674  
 1675  
 1676  
 1677 **Image Consistency Score Evaluation**  
 1678  
 1679 **Generation of Image Consistency Scores:**  
 1680 You are a professional digital artist and image evaluation specialist.  
 1681  
 1682 You will be given:  
 1683 1. **Input Image**: the original image.  
 1683 2. **Output Image**: the generated/edited image.  
 1684 3. **Input Text**: the instruction describing the intended modification.  
 1685  
 1686 **Your Objective:**  
 1687 Your task is to **evaluate the visual consistency** between the input and output images,  
 1688 focusing exclusively on elements that are **NOT** specified for change in the input text  
 1689 **instruction**. That is, you should only consider whether all non-instructed details  
 1690 remain unchanged. Do **not** penalize or reward any changes that are explicitly required  
 1691 by the instruction.  
 1692  
 1693 **## Evaluation Scale (1 to 5):**  
 1694 You will assign a **consistency\_score** according to the following rules:  
 1695 - **5 Perfect Consistency**: All non-instruction elements are completely unchanged and  
 1696 visually identical.  
 1697 - **4 Minor Inconsistency**: Only one very small, non-instruction detail is different  
 1698 (e.g., a tiny accessory, a subtle shadow, or a minor background artifact).  
 1699 - **3 Noticeable Inconsistency**: One clear non-instruction element is changed (e.g., a  
 1700 different hairstyle, a shifted object, or a visible background alteration).  
 1701 - **2 Significant Inconsistency**: Two or more non-instruction elements have been  
 1702 noticeably altered.  
 1703 - **1 Severe Inconsistency**: Most or all major non-instruction details are different  
 1704 (e.g., changed identity, gender, or overall scene layout).  
 1705  
 1706 **## Guidance:**  
 1707 - First, **identify all elements** that the input text instruction explicitly allows or  
 1708 requires to be **changed**. Exclude these from your consistency check.  
 1709 - For all other elements (e.g., facial features, clothing, background, object positions,  
 1710 colors, lighting, scene composition, etc.), **compare the output image to the input**  
 1711 **image** and check if they remain visually identical.  
 1712 - If you observe any change in a non-instruction element, note it and consider its **impact**  
 1713 on the score.  
 1714 - If the instruction is vague or ambiguous, make a best-effort factual inference about  
 1715 which elements are intended to change, and treat all others as non-instruction elements.  
 1716  
 1717 **## Note:**  
 1718 - **Do not penalize changes** that are required by the instruction.  
 1719 - **Do not reward or penalize** the quality or correctness of the instructed change  
 1720 **itself** (that is evaluated separately).  
 1721 - If the output image introduces new artifacts, objects, or changes to non-instruction  
 1722 elements, this should lower the consistency score.  
 1723  
 1724 **## Output Format**  
 1725 First, clearly explain your comparison process: list each major non-instruction element  
 1726 and state whether it is consistent (unchanged) or inconsistent (changed), with brief  
 1727 reasoning.  
 1728 Then, provide your evaluation in the following JSON format:  
 1729 {{  
 1730 "reasoning": "Compared to input image, [list of non-instruction elements that changed or  
 1731 remained the same] in the output image.",  
 1732 "consistency\_score": X  
 1733 }}  
 1734  
 1735  
 1736  
 1737  
 1738  
 1739  
 1740  
 1741  
 1742  
 1743  
 1744  
 1745  
 1746  
 1747  
 1748  
 1749  
 1750  
 1751  
 1752  
 1753  
 1754  
 1755  
 1756  
 1757  
 1758  
 1759  
 1760  
 1761  
 1762  
 1763  
 1764  
 1765  
 1766  
 1767  
 1768  
 1769  
 1770  
 1771  
 1772  
 1773  
 1774  
 1775  
 1776  
 1777  
 1778  
 1779  
 1780  
 1781  
 1782  
 1783  
 1784  
 1785  
 1786  
 1787  
 1788  
 1789  
 1790  
 1791  
 1792  
 1793  
 1794  
 1795  
 1796  
 1797  
 1798  
 1799  
 1800  
 1801  
 1802  
 1803  
 1804  
 1805  
 1806  
 1807  
 1808  
 1809  
 1810  
 1811  
 1812  
 1813  
 1814  
 1815  
 1816  
 1817  
 1818  
 1819  
 1820  
 1821  
 1822  
 1823  
 1824  
 1825  
 1826  
 1827  
 1828  
 1829  
 1830  
 1831  
 1832  
 1833  
 1834  
 1835  
 1836  
 1837  
 1838  
 1839  
 1840  
 1841  
 1842  
 1843  
 1844  
 1845  
 1846  
 1847  
 1848  
 1849  
 1850  
 1851  
 1852  
 1853  
 1854  
 1855  
 1856  
 1857  
 1858  
 1859  
 1860  
 1861  
 1862  
 1863  
 1864  
 1865  
 1866  
 1867  
 1868  
 1869  
 1870  
 1871  
 1872  
 1873  
 1874  
 1875  
 1876  
 1877  
 1878  
 1879  
 1880  
 1881  
 1882  
 1883  
 1884  
 1885  
 1886  
 1887  
 1888  
 1889  
 1890  
 1891  
 1892  
 1893  
 1894  
 1895  
 1896  
 1897  
 1898  
 1899  
 1900  
 1901  
 1902  
 1903  
 1904  
 1905  
 1906  
 1907  
 1908  
 1909  
 1910  
 1911  
 1912  
 1913  
 1914  
 1915  
 1916  
 1917  
 1918  
 1919  
 1920  
 1921  
 1922  
 1923  
 1924  
 1925  
 1926  
 1927  
 1928  
 1929  
 1930  
 1931  
 1932  
 1933  
 1934  
 1935  
 1936  
 1937  
 1938  
 1939  
 1940  
 1941  
 1942  
 1943  
 1944  
 1945  
 1946  
 1947  
 1948  
 1949  
 1950  
 1951  
 1952  
 1953  
 1954  
 1955  
 1956  
 1957  
 1958  
 1959  
 1960  
 1961  
 1962  
 1963  
 1964  
 1965  
 1966  
 1967  
 1968  
 1969  
 1970  
 1971  
 1972  
 1973  
 1974  
 1975  
 1976  
 1977  
 1978  
 1979  
 1980  
 1981  
 1982  
 1983  
 1984  
 1985  
 1986  
 1987  
 1988  
 1989  
 1990  
 1991  
 1992  
 1993  
 1994  
 1995  
 1996  
 1997  
 1998  
 1999  
 2000  
 2001  
 2002  
 2003  
 2004  
 2005  
 2006  
 2007  
 2008  
 2009  
 2010  
 2011  
 2012  
 2013  
 2014  
 2015  
 2016  
 2017  
 2018  
 2019  
 2020  
 2021  
 2022  
 2023  
 2024  
 2025  
 2026  
 2027  
 2028  
 2029  
 2030  
 2031  
 2032  
 2033  
 2034  
 2035  
 2036  
 2037  
 2038  
 2039  
 2040  
 2041  
 2042  
 2043  
 2044  
 2045  
 2046  
 2047  
 2048  
 2049  
 2050  
 2051  
 2052  
 2053  
 2054  
 2055  
 2056  
 2057  
 2058  
 2059  
 2060  
 2061  
 2062  
 2063  
 2064  
 2065  
 2066  
 2067  
 2068  
 2069  
 2070  
 2071  
 2072  
 2073  
 2074  
 2075  
 2076  
 2077  
 2078  
 2079  
 2080  
 2081  
 2082  
 2083  
 2084  
 2085  
 2086  
 2087  
 2088  
 2089  
 2090  
 2091  
 2092  
 2093  
 2094  
 2095  
 2096  
 2097  
 2098  
 2099  
 2100  
 2101  
 2102  
 2103  
 2104  
 2105  
 2106  
 2107  
 2108  
 2109  
 2110  
 2111  
 2112  
 2113  
 2114  
 2115  
 2116  
 2117  
 2118  
 2119  
 2120  
 2121  
 2122  
 2123  
 2124  
 2125  
 2126  
 2127  
 2128  
 2129  
 2130  
 2131  
 2132  
 2133  
 2134  
 2135  
 2136  
 2137  
 2138  
 2139  
 2140  
 2141  
 2142  
 2143  
 2144  
 2145  
 2146  
 2147  
 2148  
 2149  
 2150  
 2151  
 2152  
 2153  
 2154  
 2155  
 2156  
 2157  
 2158  
 2159  
 2160  
 2161  
 2162  
 2163  
 2164  
 2165  
 2166  
 2167  
 2168  
 2169  
 2170  
 2171  
 2172  
 2173  
 2174  
 2175  
 2176  
 2177  
 2178  
 2179  
 2180  
 2181  
 2182  
 2183  
 2184  
 2185  
 2186  
 2187  
 2188  
 2189  
 2190  
 2191  
 2192  
 2193  
 2194  
 2195  
 2196  
 2197  
 2198  
 2199  
 2200  
 2201  
 2202  
 2203  
 2204  
 2205  
 2206  
 2207  
 2208  
 2209  
 2210  
 2211  
 2212  
 2213  
 2214  
 2215  
 2216  
 2217  
 2218  
 2219  
 2220  
 2221  
 2222  
 2223  
 2224  
 2225  
 2226  
 2227  
 2228  
 2229  
 2230  
 2231  
 2232  
 2233  
 2234  
 2235  
 2236  
 2237  
 2238  
 2239  
 2240  
 2241  
 2242  
 2243  
 2244  
 2245  
 2246  
 2247  
 2248  
 2249  
 2250  
 2251  
 2252  
 2253  
 2254  
 2255  
 2256  
 2257  
 2258  
 2259  
 2260  
 2261  
 2262  
 2263  
 2264  
 2265  
 2266  
 2267  
 2268  
 2269  
 2270  
 2271  
 2272  
 2273  
 2274  
 2275  
 2276  
 2277  
 2278  
 2279  
 2280  
 2281  
 2282  
 2283  
 2284  
 2285  
 2286  
 2287  
 2288  
 2289  
 2290  
 2291  
 2292  
 2293  
 2294  
 2295  
 2296  
 2297  
 2298  
 2299  
 2300  
 2301  
 2302  
 2303  
 2304  
 2305  
 2306  
 2307  
 2308  
 2309  
 2310  
 2311  
 2312  
 2313  
 2314  
 2315  
 2316  
 2317  
 2318  
 2319  
 2320  
 2321  
 2322  
 2323  
 2324  
 2325  
 2326  
 2327  
 2328  
 2329  
 2330  
 2331  
 2332  
 2333  
 2334  
 2335  
 2336  
 2337  
 2338  
 2339  
 2340  
 2341  
 2342  
 2343  
 2344  
 2345  
 2346  
 2347  
 2348  
 2349  
 2350  
 2351  
 2352  
 2353  
 2354  
 2355  
 2356  
 2357  
 2358  
 2359  
 2360  
 2361  
 2362  
 2363  
 2364  
 2365  
 2366  
 2367  
 2368  
 2369  
 2370  
 2371  
 2372  
 2373  
 2374  
 2375  
 2376  
 2377  
 2378  
 2379  
 2380  
 2381  
 2382  
 2383  
 2384  
 2385  
 2386  
 2387  
 2388  
 2389  
 2390  
 2391  
 2392  
 2393  
 2394  
 2395  
 2396  
 2397  
 2398  
 2399  
 2400  
 2401  
 2402  
 2403  
 2404  
 2405  
 2406  
 2407  
 2408  
 2409  
 2410  
 2411  
 2412  
 2413  
 2414  
 2415  
 2416  
 2417  
 2418  
 2419  
 2420  
 2421  
 2422  
 2423  
 2424  
 2425  
 2426  
 2427  
 2428  
 2429  
 2430  
 2431  
 2432  
 2433  
 2434  
 2435  
 2436  
 2437  
 2438  
 2439  
 2440  
 2441  
 2442  
 2443  
 2444  
 2445  
 2446  
 2447  
 2448  
 2449  
 2450  
 2451  
 2452  
 2453  
 2454  
 2455  
 2456  
 2457  
 2458  
 2459  
 2460  
 2461  
 2462  
 2463  
 2464  
 2465  
 2466  
 2467  
 2468  
 2469  
 2470  
 2471  
 2472  
 2473  
 2474  
 2475  
 2476  
 2477  
 2478  
 2479  
 2480  
 2481  
 2482  
 2483  
 2484  
 2485  
 2486  
 2487  
 2488  
 2489  
 2490  
 2491  
 2492  
 2493  
 2494  
 2495  
 2496  
 2497  
 2498  
 2499  
 2500  
 2501  
 2502  
 2503  
 2504  
 2505  
 2506  
 2507  
 2508  
 2509  
 2510  
 2511  
 2512  
 2513  
 2514  
 2515  
 2516  
 2517  
 2518  
 2519  
 2520  
 2521  
 2522  
 2523  
 2524  
 2525  
 2526  
 2527  
 2528  
 2529  
 2530  
 2531  
 2532  
 2533  
 2534  
 2535  
 2536  
 2537  
 2538  
 2539  
 2540  
 2541  
 2542  
 2543  
 2544  
 2545  
 2546  
 2547  
 2548  
 2549  
 2550  
 2551  
 2552  
 2553  
 2554  
 2555  
 2556  
 2557  
 2558  
 2559  
 2560  
 2561  
 2562  
 2563  
 2564  
 2565  
 2566  
 2567  
 2568  
 2569  
 2570  
 2571  
 2572  
 2573  
 2574  
 2575  
 2576  
 2577  
 2578  
 2579  
 2580  
 2581  
 2582  
 2583  
 2584  
 2585  
 2586  
 2587  
 2588  
 2589  
 2590  
 2591  
 2592  
 2593  
 2594  
 2595  
 2596  
 2597  
 2598  
 2599  
 2600  
 2601  
 2602  
 2603  
 2604  
 2605  
 2606  
 2607  
 2608  
 2609  
 2610  
 2611  
 2612  
 2613  
 2614  
 2615  
 2616  
 2617  
 2618  
 2619  
 2620  
 2621  
 2622  
 2623  
 2624  
 2625  
 2626  
 2627  
 2628  
 2629  
 2630  
 2631  
 2632  
 2633  
 2634  
 2635  
 2636  
 2637  
 2638  
 2639  
 2640  
 2641  
 2642  
 2643  
 2644  
 2645  
 2646  
 2647  
 2648  
 2649  
 2650  
 2651  
 2652  
 2653  
 2654  
 2655  
 2656  
 2657  
 2658  
 2659  
 2660  
 2661  
 2662  
 2663  
 2664  
 2665  
 2666  
 2667  
 2668  
 2669  
 2670  
 2671  
 2672  
 2673  
 2674  
 2675  
 2676  
 2677  
 2678  
 2679  
 2680  
 2681  
 2682  
 2683  
 2684  
 2685  
 2686  
 2687  
 2688  
 2689  
 2690  
 2691  
 2692  
 2693  
 2694  
 2695  
 2696  
 2697  
 2698  
 2699  
 2700  
 2701  
 2702  
 2703  
 2704  
 2705  
 2706  
 2707  
 2708  
 2709  
 2710  
 2711  
 2712  
 2713  
 2714  
 2715  
 2716  
 2717  
 2718  
 2719  
 2720  
 2721  
 2722  
 2723  
 2724  
 2725  
 2726  
 2727  
 2728  
 2729  
 2730  
 2731  
 2732  
 2733  
 2734  
 2735  
 2736  
 2737  
 2738  
 2739  
 2740  
 2741  
 2742  
 2743  
 2744  
 2745  
 2746  
 2747  
 2748  
 2749  
 2750  
 2751  
 2752  
 2753  
 2754  
 2755  
 2756  
 2757  
 2758  
 2759  
 2760  
 2761  
 2762  
 2763  
 2764  
 2765  
 2766  
 2767  
 2768  
 2769  
 2770  
 2771  
 2772  
 2773  
 2774  
 2775  
 2776  
 2777  
 2778  
 2779  
 2780  
 2781  
 2782  
 2783  
 2784  
 2785  
 2786  
 2787  
 2788  
 2789  
 2790  
 2791  
 2792  
 2793  
 2794  
 2795  
 2796  
 2797  
 2798  
 2799  
 2800  
 2801  
 2802  
 2803  
 2804  
 2805  
 2806  
 2807  
 2808  
 2809  
 2810  
 2811  
 2812  
 2813  
 2814  
 2815  
 2816  
 2817  
 2818  
 2819  
 2820  
 2821  
 2822  
 2823  
 2824  
 2825  
 2826  
 2827  
 2828  
 2829  
 2830  
 2831  
 2832  
 2833  
 2834  
 2835  
 2836  
 2837  
 2838  
 2839  
 2840  
 2841  
 2842  
 2843  
 2844  
 2845  
 2846  
 2847  
 2848  
 2849  
 2850  
 2851  
 2852  
 2853  
 2854  
 2855  
 2856  
 2857  
 2858  
 2859  
 2860  
 2861  
 2862  
 2863  
 2864  
 2865  
 2866  
 2867  
 2868  
 2869  
 2870  
 2871  
 2872  
 2873  
 2874  
 2875  
 2876  
 2877  
 2878  
 2879  
 2880  
 2881  
 2882  
 2883  
 2884  
 2885  
 2886  
 2887  
 2888  
 2889  
 2890  
 2891  
 2892  
 2893  
 2894  
 2895  
 2896  
 2897  
 2898  
 2899  
 2900  
 2901  
 2902  
 2903  
 2904  
 2905  
 2906  
 2907  
 2908  
 2909  
 2910  
 2911  
 2912  
 2913  
 2914  
 2915  
 2916  
 2917  
 2918  
 2919  
 2920  
 2921  
 2922  
 2923  
 2924  
 2925  
 2926  
 2927  
 2928  
 2929  
 2930  
 2931  
 2932  
 2933  
 2934  
 2935  
 2936  
 2937  
 2938  
 2939  
 2940  
 2941  
 2942  
 2943  
 2944  
 2945  
 2946  
 2947  
 2948  
 2949  
 2950  
 2951  
 2952  
 2953  
 2954  
 2955  
 2956  
 2957  
 2958  
 2959  
 2960  
 2961  
 2962  
 2963  
 2964  
 2965  
 2966  
 2967  
 2968  
 2969  
 2970  
 2971  
 2972  
 2973  
 2974  
 2975  
 2976  
 2977  
 2978  
 2979  
 2980  
 2981  
 2982  
 2983  
 2984  
 2985  
 2986  
 2987  
 2988  
 2989  
 2990  
 2991  
 2992  
 2993  
 2994  
 2995  
 2996<br

1728  
 1729  
 1730  
 1731     **Image Quality Score Evaluation**  
 1732  
 1733     **Generation of Image Quality Scores:**  
 1734     You are a professional digital artist and image evaluation specialist.  
 1735  
 1736     You will be given:  
 1737       - **Output Image**: an AI-generated image.  
 1738  
 1739     **## Objective:**  
 1740     Your task is to **evaluate the perceptual quality** of the output image, focusing on:  
 1741       - **Structural and semantic coherence**  
 1742       - **Natural appearance**  
 1743       - **Absence of generation artifacts**  
 1744       - **Visual clarity and composition**  
 1745  
 1746     You must **not penalize low resolution or moderate softness** unless it introduces  
 1747     semantic ambiguity or visually degrading effects.  
 1748  
 1749     **## Evaluation Scale (1 to 5):**  
 1750     You will assign a **quality\_score** with the following rule:  
 1751  
 1752       - **5 Excellent Quality**: All aspects are visually coherent, natural, and free from  
 1753       noticeable artifacts. Structure, layout, and textures are accurate and consistent. The  
 1754       image has clear composition and professional appearance.  
 1755       - **4 Minor Issues**: One small imperfection (e.g., slight texture blending, minor  
 1756       lighting inconsistency, small compositional flaw).  
 1757       - **3 Noticeable Artifacts**: One or two clear visual flaws or semantic problems (e.g.,  
 1758       extra fingers, minor duplication, slight distortion, unnatural lighting).  
 1759       - **2 Structural Degradation**: Multiple distracting errors (e.g., melted hands, warped  
 1760       shapes, unreadable text, poor composition, obvious artifacts).  
 1761       - **1 Severe Errors**: Major structural failures or hallucinations (e.g., broken anatomy,  
 1762       garbled symbols, severe distortions, completely unnatural appearance).  
 1763  
 1764     **## Guidance:**  
 1765     Check the following visual aspects and mark them as **✓** (satisfactory) or **X** (problematic):  
 1766       - **Structural coherence**: Correct anatomy, object shapes, legible text, proper  
 1767       proportions  
 1768       - **Natural appearance**: Realistic lighting, perspective, shadow logic, believable  
 1769       textures  
 1770       - **Artifact-free**: No duplication, ghosting, watermarks, obvious generation artifacts  
 1771       - **Texture fidelity**: Clothing, hair, surfaces not melted or corrupted  
 1772       - **Composition**: Clear focal points, balanced elements, appropriate framing  
 1773       - **Color harmony**: Natural color relationships, appropriate saturation and contrast  
 1774  
 1775     **✓ The more checks, the higher the score.**  
 1776  
 1777     **## Output Format:**  
 1778     After evaluation, provide your score and concise reasoning using the following JSON  
 1779     format:  
 1780     {{  
 1781       "quality\_score": X,  
 1782       "reasoning": "Structural coherence: ✓/X, Natural appearance: ✓/X, Artifacts: ✓/X,  
 1783       Texture fidelity: ✓/X, Composition: ✓/X, Color harmony: ✓/X. [Brief explanation of  
 1784       key issues or strengths]"  
 1785     }}  
 1786  
 1787  
 1788  
 1789  
 1790  
 1791

Figure 20: Image quality evaluation prompt

1782  
 1783  
 1784  
 1785     **Image Alignment Score Evaluation**  
 1786  
 1787     **Generation of Image Instruction Following Scores:**  
 1788     You are a professional digital artist and image evaluation specialist. You will evaluate  
       the effectiveness of the AI-generated image based on given rules.  
 1789  
 1790     You will be given:  
 1791       1. **Input Image**: the original image.  
 1792       2. **Output Image**: the generated/edited image.  
 1793       3. **Input Text**: the instruction describing the intended modification.  
 1794  
 1795     Your Objective:  
 1796     Your task is to **evaluate how the output image faithfully fulfills the input text instruction**, focusing **exclusively on the presence and correctness of the specified changes**.  
 1797  
 1798     You must:  
 1799       - **Identify detailed visual differences** between Input Image and Output Image **correctly and faithfully**.  
 1800       - Determine if those differences **match exactly what the input text instruction requests**  
 1801       - **Not assess any unintended modifications beyond the instruction**; such evaluations fall under separate criteria.  
 1802       - **Be careful**, an edit may introduce visual change without fulfilling the actual instruction (e.g., replacing the object instead of modifying it)  
 1803  
 1804  
 1805     ## Reasoning:  
 1806     You must follow these reasoning steps before scoring:  
 1807       **1. Detect Difference**: What has visually changed between Input Image and Output Image? (e.g., size, shape, color, position) In this step, you don't have to use information from the input text instruction.  
 1808  
 1809       **2. Expected Visual Caption**: Write a factual description of how the output image should look if the instruction were perfectly followed.  
 1810  
 1811       **3. Instruction Match**:  
 1812       Compare the observed differences in **1** to the expected change in **2**:  
 1813       - Was the correct object modified (not replaced)?  
 1814       - Was the requested attribute (e.g., size, color, position) modified as intended?  
 1815       - Is the degree of modification accurate (e.g., "match size," "slightly increase," etc.)?  
 1816       **4. Decision**: Use the 1-5 scale to assign a final score.  
 1817  
 1818     ## Evaluation Scale (1 to 5):  
 1819     You will assign an **instruction\_score** with following rule:  
 1820       - **5 Perfect Compliance**: The output image **precisely matches** the intended modification; all required changes are present and accurate.  
 1821       - **4 Minor Omission**: The core change is made, but **minor detail** is missing or slightly incorrect.  
 1822       - **3 Partial Compliance**: The main idea is present, but one or more required aspects are wrong or incomplete.  
 1823       - **2 Major Omission**: Most of the required changes are missing or poorly implemented.  
 1824       - **1 Non-Compliance**: The instruction is **not followed at all** or is **completely misinterpreted**  
 1825  
 1826     ## Output Format  
 1827     Look at the input again, provide the evaluation score and the explanation in the following JSON format:  
 1828       {  
 1829        "instruction\_score": X,  
 1830        "reasoning": "1. Detect Difference: ... 2. Expected Visual Caption: ... 3. Instruction Match: ... 4. Decision: ..."  
 1831       }  
 1832  
 1833     Figure 21: Image alignment evaluation prompt  
 1834  
 1835